Journal of Chromatography, 506 (1990) 495–545
Elsevier Science Publishers B.V., Amsterdam — Printed in The Netherlands

CHROMSYMP. 1707

Solutions of the equilibrium and semi-equilibrium models of chromatography

SADRODDIN GOLSHAN-SHIRAZI and GEORGES GUIOCHON*
**Department of Chemistry, University of Tennessee, Knoxville, TN 37996-1600 and Division of Analytical Chemistry, Oak Ridge National Laboratory, Oak Ridge, TN (U.S.A.)*

SUMMARY

In contrast to the kinetic models, the ideal and semi-ideal models of chromatography assume the distribution of the compounds studied to be constantly at equilibrium (ideal model) or very close to equilibrium (semi-ideal model). An exact solution of the ideal model can be obtained under close form for a pure compound with any isotherm and for a binary mixture with competitive Langmuir isotherms. No exact solution of the semi-ideal model can be derived but numerical solutions are available for all isotherms. Approximate analytical solutions for this model can be obtained by assuming that the concentration of the compound studied in the mobile phase is small and, accordingly, that the equilibrium isotherm is parabolic and by neglecting some terms in the derivation. Depending on the assumptions made, the Houghton and the Haarhoff–Van der Linde equations are obtained.

These different solutions are compared. It is shown that the Haarhoff–Van der Linde equation is a much better approximation than the Houghton equation and that its range of validity depends essentially on the deviation between the true isotherm and its two-term expansion in the concentration range sampled by the band during its elution. It is usually valid for loading factors below 0.2% for an ideal column and $bC_{Max} \leq 0.05$ for real columns (the loading factor is the ratio of the sample size and the column saturation capacity, b is the second coefficient of a Langmuir isotherm and C_{Max} is the maximum concentration of the band). In practice, however, it can be used for loading factors up to 1% ($bC_{Max} \leq 0.1$ for real columns). The ideal model, in contrast, gives a valid presentation of experimental band profiles only at high sample size and column efficiencies. The reduced sample size, $m = N L_f [k'_0/(1 + k'_0)]^2$ (N = column plate number, L_f = loading factor, k'_0 = column capacity factor), must be higher than 35. In the intermediate range, only numerical solutions can predict the band profiles accurately.

In the case of two components, the exact solution of the ideal model can be obtained under close form with competitive Langmuir isotherms. Numerical solutions can be obtained to simulate real columns. No other analytical solution, even approximate, is available. A correction made to the ideal model to account for the band-broadening effect of a finite efficiency gives good results and permits the in-

0021-9673/90/$03.50

vestigation of the optimization of the experimental conditions of a separation for maximum production rate.

INTRODUCTION

Because of the importance recently acquired by preparative chromatography as a separation technique for the industrial extraction and purification of synthesis intermediates and of products in biotechnology, there is renewed interest in fundamental chromatography. In order to optimize a separation process, we need to be able to predict its results. In the case of preparative chromatography, we want an accurate prediction of the concentration signal observed at the outlet of the column as a function of the experimental parameters and of the initial and boundary conditions.

The derivation of accurate predictions requires the use of a sophisticated model. Such a model can rarely be solved exactly by an analytical solution, *i.e.*, in closed form. Approximations may be necessary or numerical solutions may be calculated. The former can be differentiated and the optimum conditions for maximum production rate under any combination of constraints regarding collected fraction purity and component recovery yield can be derived in a straightforward way. The latter have the advantage of being accurate, calculable with the required precision and available for almost any combination of the experimental parameters, but they require the selection of the proper numerical value for each parameter involved. Further, optimization is difficult to carry out using the numerical approach, as it needs repetitive calculations of chromatograms, for a long series of sets of variable experimental parameters.

Therefore, analytical solutions are highly desirable in order to investigate in detail the influence on the production rate of the column length, the size of the packing particles, the mobile phase flow velocity and composition, *i.e.*, the selectivity of the phase system, the non-linear behavior of the isotherm, the sample size and relative composition, the axial dispersion and the kinetics of radial mass transfer. Analytical solutions are so useful that we are ready to sacrifice some accuracy, make simplifying assumptions, in order to formulate a model which can be resolved into closed forms. It is important to know, however, what the importance of the error made in these simpler models is and the extent to which the profiles they predict for the concentration signal at the column exit deviate from the true profiles. The aim of this paper is to review the various analytical solutions that have been derived, assuming that the chromatographic phase system is constantly at equilibrium or very near it (*i.e.*, high column efficiency). In forthcoming papers, we shall present a similar investigation of the kinetic models of chromatography and a comparison between semi-equilibrium and kinetic models[1].

Although separation methods, and chromatography in particular, concern the extraction and purification of certain components of mixtures, the main thrust of this work will be on the prediction of the elution profile of pure compounds. There are several modes under which chromatography can be carried out, *e.g.*, isocratic, step and gradient elution, frontal analysis and displacement, but most of the theoretical effort has dealt with isocratic elution. More importantly, the difficulties with the two-component problem are such that very few papers have discussed it.

EQUILIBRIUM AND SEMI-EQUILIBRIUM MODELS

The most general approach to chromatography is a model which expresses that the mass of each component in the column is constant and relates the rate of mass transfer of each component to the local composition of the chromatographic system. The former condition is easy to write, and is called the mass balance equation. The theoretical difficulties begin with the formulation of the second set of equations, as kinetics are much more complicated than thermodynamics. Various equations, with different merits and drawbacks, have been written, which will be reviewed later[1]. Because it has long been recognized that the mass transfer in the non-consolidated beds of porous particles used in chromatographic columns are usually very fast and that in most instances these columns are operated near equilibrium, a very popular and very fruitful approach is to assume, in a first step, that the mass transfer is infinitely fast and the column efficiency infinite. Then a perturbative correction is made, to take that efficiency into account. Another approach, equally fruitful, but for a different range of sample sizes, is to lump the coefficients of radial mass transfers into a coefficient of apparent axial dispersion and to consider the effect of a large concentration either as negligible (linear chromatography) or as a perturbation. Both approaches are, of course, doomed to failure when the mass transfer kinetics are very slow.

Before discussing these different approaches, we review first the basic equations of the model and the rationale for the development of the equilibrium and semi-equilibrium models (*i.e.*, the ideal and semi-ideal models).

Mass balance equation

This equation was derived by Wilson[2], 50 years ago. It states that the amount of a component which enters an infinitely thin slice of column in an infinitely short period of time is equal to the sum of what leaves the slice and what remains in it. It is written as

$$\frac{\partial C}{\partial t} + F\frac{\partial C_s}{\partial t} + u\frac{\partial C}{\partial z} = D\frac{\partial^2 C}{\partial z^2} \tag{1}$$

where C_s and C are the concentrations of the studied compound in the stationary and the mobile phase, respectively; z and t are the abscissa along the column (assumed to be one-dimensional) and time, respectively; u is the mobile phase velocity; F is the phase ratio, $(1 - \varepsilon)/\varepsilon$, where ε is the packing porosity, and D is the coefficient of axial dispersion, which includes the axial molecular diffusion, the packing tortuosity and the contribution of packing heterogeneity to the band dispersion.

The conditions under which this equation is a valid mass balance (non-compressible mobile phase, constant diffusion coefficient, constant partial molar volume of the solute and no sorption effect) have been discussed in previous publications and are not seriously restrictive[3]. An equation such as eqn. 1 should be written for each component of the system, except the mobile phase when it is pure or the weakest component of this phase[4,5]. In practice, however, when the mobile phase is a mixed solvent and the strong components or additives of this solution are much less strongly adsorbed than the component of the sample, the mass balances of the components of the mobile phase can be neglected, provided that the isotherm of the sample components are measured by reference to the mobile phase[4]. This simplification is

valid as long as the column capacity factors of the mobile phase components at infinite dilution in the pure weak solvent are at least five times smaller than the column capacity factors of the sample components.

Kinetic equation

Eqn. 1 contains two functions of z and t, the concentrations of the studied compound in the stationary and the mobile phase. In order to solve this equation, we need a relationship between these two concentrations. Should we be able to formulate it, a kinetic equation can provide the needed intermediate.

A more detailed discussion of this problem will be presented in a forthcoming paper[1]. Suffice it to say here that among the models which have been used to describe such kinetics, the three simplest are the following (in these equations, C_s is the local concentration of component in the stationary phase, q, the concentration in equilibrium with C in the mobile phase):

The Langmuir kinetics model:

$$\frac{\partial C_s}{\partial t} = k_a(q_s - C_s)C - k_d C_s \tag{2}$$

where q_s is the column saturation capacity (in the same units as C_s) and k_a and k_d are the adsorption and desorption rate constants of the compound, respectively. This equation has been used by Thomas[6], Goldstein[7] and later by Wade *et al.*[8].

The linear kinetics model:

$$\frac{\partial C_s}{\partial t} = k_1 C - k_2 C_s \tag{3}$$

where k_1 and k_2 are rate constants, which has been used by Lapidus and Amundson[9].

The linear driving force model:

$$\frac{\partial C_s}{\partial t} = k_f(q - C_s) \tag{4}$$

where q is the equilibrium value of C_s, when the mobile phase concentration is C (see discussion of the equilibrium isotherm, next section), and k_f is the lumped mass transfer coefficient. Eqn. 4 has been used by Glueckauf[10], Hiester and Vermeulen[11] and later by Lin *et al.*[12] and Golshan-Shirazi *et al.*[13]. In linear chromatography (infinitely small sample size), this last model is a particular case of the linear kinetics model ($q = k'_0 C$, $k_f k'_0 = k_1$, $k_f = k_2$).

The properties, advantages and drawbacks of these models are discussed elsewhere, together with the characteristics of their solutions[1].

Initial and boundary conditions

All chromatographic problems can be solved by using the appropriate system of eqns. 1 and 2, 3 or 4, *i.e.*, the system composed of as many equations of either group as there are components involved in the system being studied. The solution, $C(z,t)$, the

concentration of the compound in the eluent at position z and time t, is determined, however, only when the initial and the boundary conditions are selected. The proper choice of these conditions permits the prediction of elution (constant mobile phase composition at column inlet, pulse injection), gradient elution (pulse injection, followed by pumping a mobile phase which is a ramp of strong solvent), displacement [column initially filled with a mobile phase, pulse injection, followed by the injection of a concentration plateau of a displacer (*i.e.*, a strongly retained compound) in the mobile phase], frontal analysis (injection of a concentration plateau of sample in the mobile phase, into a column filled with pure mobile phase). More complex boundary conditions can be easily derived to simulate sophisticated experiments.

In the most popular mode used in preparative chromatography, elution, the initial conditions correspond to a column filled with pure solvent:

$$C(z,0) = 0 \tag{5a}$$

and the boundary conditions correspond to a rectangular pulse injection of duration t_p and height C_0:

$$C(0,t) = C_0 \qquad 0 < t \leqslant t_p \tag{5b}$$

and:

$$C(0,t) = 0 \qquad t_p < t \tag{5c}$$

Semi-equilibrium model in linear chromatography

In the case of a linear isotherm, Lapidus and Amundson[9] derived an analytical solution of the system of partial differential equations combining the mass balance equation and a first-order mass transfer kinetic equation. This solution is valid only in analytical applications of chromatography, because of the limitation introduced by the assumption of a linear isotherm.

Van Deemter *et al.*[14] were able to demonstrate that, when the sum of the mixing stage ($2D/u$) and the height of the mass transfer stage $[2uk'_0/(1 + k'_0)^2k_f]$ is much smaller than the column length, L, the analytical solution derived by Lapidus and Amundson reduces to a Gaussian profile (k'_0 is the column capacity factor and k_f the lumped mass transfer coefficient of eqn. 4). In this case, the exact analytical solution of Lapidus and Amundson is equivalent to the solution of the simplified plate theory of Martin and Synge[15]. The Van Deemter equation provides the equivalence by relating the standard deviation of the Gaussian profile to which the solution of the Lapidus and Amundson equation reduces and the standard deviation of the plate model, through the value of the column plate height[14]:

$$H = \frac{2D}{u} + \frac{2uk'_0}{(1 + k'_0)^2 k_f} \tag{6}$$

When the experimental conditions are such that the plate height increases to the point that it is no longer much smaller than the column length, the plate theory fails, and the

more general solution of Lapidus and Amundson must be used for an accurate prediction of the band profile.

Still within the framework of linear chromatography, Kucera[16] derived the solution of the most general model of chromatography, with a mass balance including axial dispersion and kinetic equations including the contributions to the resistance to radial mass transfers which are due to diffusion across the boundary film between the mobile and the stagnant mobile phase, to intraparticle diffusion and to first-order reaction kinetics for the retention mechanism. This solution, however, is in closed form in the Laplace domain only, and it cannot be converted into the time domain. When the elution profile is Gaussian, comparison between the values of the second moment predicted by the general diffusion model and by the linear driving force model shows that the lumped mass transfer coefficient is related to the pore diffusion and the film mass transfer resistance by the following equation:

$$\frac{F}{k'_0 k_f} = \frac{d_p}{6k_e} + \frac{d_p^2}{60\beta D_p} \tag{7}$$

where d_p is the average particle size, k_e is the external film mass transfer coefficient, F is the phase ratio, β is the inner porosity of the packing particles and D_p is the intraparticle diffusion coefficient.

Horvath and Lin[17] and Huber[18] derived relationships between the parameters of sophisticated mass transfer models and the column plate height. As often occurs in physical chemistry, difficulties arise when complex models have to be compared with experimental data, as the multiplication of the parameters introduced in the models in an effort to make them more exact increases arbitrarily the flexibility of the overall equation and at the same time makes the proper estimate of the various parameters more difficult and the final values less reliable.

The problem becomes much more complicated when the isotherm is not linear. There is no general analytical solution available which could compare with the solution of Lapidus and Amundson and could provide a tool for the investigation of column performance which would be as powerful and as general as the column HETP.

Semi-equilibrium model in non-linear chromatography

In his non-equilibrium theory, Giddings[19] attempted to relate the band broadening due to the resistances to radial mass transfer and the experimental parameters. Central to this theoretical development is the assumption that the two phases of a chromatographic system are always close to equilibrium. This is certainly true in all modern, high-performance chromatographic techniques. The only possible exceptions are some implementations of ion-exchange chromatography and most applications of affinity chromatography, as the dissociation of the selective recognition complex is generally a slow process.

For the sake of simplicity, the concentrations in this subsection are referred to the total column volume, and not to the volumes of either mobile or stationary phases. We denote by $\bar{C}^*$ an equilibrium concentration and by $\bar{C}$ an actual concentration. We can write

$$\bar{C}_m = \bar{C}_m^*(1 + \varepsilon_m) \tag{8a}$$

and

$$\bar{C}_s = \bar{C}_s^*(1 + \varepsilon_s) \tag{8b}$$

where ε_m and ε_s account for the departure from equilibrium. These quantities are small, since the system is always near equilibrium. This is because, although the concentration gradients may be large at times, they apply only over very short distances. ε_m and ε_s are related through

$$\varepsilon_m \bar{C}_m^* + \varepsilon_s \bar{C}_s^* = 0 \tag{9}$$

Now, ignoring the longitudinal, diffusionel flux in the stationary phase, which is negligible, the flux of a compound, J, per unit column cross-sectional area, is

$$J = u\bar{C}_m = u\bar{C}_m^* + u\bar{C}_m^*\varepsilon_m \tag{10}$$

The second term in this equation, $\Delta J = u\bar{C}_m^*\varepsilon_m$, results from non-equilibrium. It is formally equivalent to a diffusion term, with a pseudo-diffusion coefficient $\acute{D}$, given by

$$D' = \frac{-\Delta J}{\partial\bar{C}/\partial z} = \frac{-u\bar{C}_m^*\varepsilon_m}{\partial\bar{C}/\partial z} \tag{11}$$

in accordance with Fick's law, where $\bar{C}$ is the total solute concentration, hence $\bar{C}_m^* = R\bar{C}$, R being the fraction of solute in the mobile phase, *i.e.*, $1/(1 + k'_0)$.

The beauty of this equation is that it shows that non-equilibrium effects, which result from lateral diffusion, can be treated as a contribution to axial dispersion. Accordingly, we can describe the chromatographic phenomenon by keeping the mass balance equation (eqn. 1), eliminate the kinetic equation from the system, replace the concentration in the stationary phase C_s in eqn. 1 by the value given by the equilibrium isotherm, $q = f(C)$, and replace the axial dispersion coefficient, D, by an apparent axial dispersion coefficient, related to the column HETP by $D_a = HL/2t_0$ (ref. 3).

Haarhoff and Van der Linde[20] have given a more general demonstration of this result, which is valid for a slightly overloaded column, with a parabolic isotherm. It leads to the following equation for the mass balance of a compound:

$$\frac{\partial C}{\partial t} + F\frac{\partial q}{\partial t} + u\frac{\partial C}{\partial x} = D_a\frac{\partial^2 C}{\partial z^2} \tag{12}$$

where q is the concentration of the solute in the stationary phase in equilibrium with the concentration, C, in the mobile phase, given by the isotherm equation:

$$q = f(C) \tag{13}$$

We shall discuss later the validity of this assumption and show in which range of column efficiency the semi-equilibrium model is an accurate chromatographic model[1].

Equilibrium model

If we assume that there is no axial dispersion and that the kinetics of radial mass transfer are infinitely fast, the mobile and the stationary phases are constantly at equilibrium. Then the mass balance of the compound studied (eqn. 1) becomes

$$u\frac{\partial C}{\partial z} + \left(1 + F\frac{dq}{dC}\right)\frac{\partial C}{\partial t} = 0 \tag{14}$$

Eqn. 14 was the form under which the mass balance was derived originally by Wilson[2], who also investigated its properties, but did not realize the possibility of the formation of shock or concentration discontinuities, which eqn. 14 can propagate as shown later by DeVault[21] and as discussed recently by Lin *et al.*[22]. Thus, Wilson[2] concluded that the band width remains constant during the band migration, which is true only under linear conditions. Later, the problem was rediscussed by Weiss[23] and more rigorously by DeVault[21], who explained the formation and propagation of concentration discontinuities. Glueckauf[24] extended the theoretical results of DeVault to the case of a sigmoidal isotherm.

The solution of the ideal model of chromatography has been intensively discussed in the past, notably by Glueckauf[24–26], Amundson and co-workers[27,28] and Guiochon and co-workers[29,30]. Recently, an analytical solution has been formulated for the single-component problem in the case of a Langmuir isotherm[31] and in the general case of any isotherm[32]. An analytical solution has also been demonstrated for a two-component mixture, when the equilibrium isotherms of the two components are given by the classical competitive Langmuir model[33,34]. These solutions will be discussed and compared with the approximate analytical solutions and with the numerical solutions of the semi-ideal model[3,35].

ANALYTICAL SOLUTIONS OF THE IDEAL AND SEMI-IDEAL MODEL FOR A SINGLE COMPOUND

Four main solutions are available for the prediction of the elution profile of a pure compound on an overloaded chromatographic column. These equations are the analytical solution of the ideal model[32], two approximate solutions of the semi-ideal model, suggested by Houghton[36] and Haarhoff and Van der Linde[20], and the numerical solution of the semi-ideal model[3]. In contrast to the ideal model solution, which neglects the kinetic effect on the band profile, the two approximate analytical solutions of the semi-ideal model consider the kinetic effect as important, and the non-linear or thermodynamic effect as a perturbation for which they account. The numerical solution of the semi-ideal model takes both thermodynamic and kinetic effects into full account.

Analytical solution of the ideal model

In a previous study[32], we derived general equations which predict the elution band profile of a large size sample of a compound for which the isotherm has no inflection point in the concentration range sampled by the band. In the case of a convex

upward isotherm, the profile of the rear, diffuse part of the band is given by the following equation:

$$t = t_p + t_0\left(1 + F\frac{dq}{dC}\right) \tag{15}$$

where F is the phase ratio. If the isotherm is convex downward, the same equation applies, but it gives the profile of the diffuse front. The profile ends (for a convex upward isotherm) at time

$$t = t_p + t_{R,0} \tag{16}$$

The retention time of the band front can be calculated by observing that, as the sample mass is constant, the area under the profile given by eqn. 15, between the retention time of the front, t_R, and the end of the profile, is equal to the sample size in chromatographic units, *i.e.*, to the product of the concentration, C_0 of the pulse injected and its width, t_p, or to the ratio of the sample size (n in moles) to the volume flow-rate, F_v. Hence, the front retention time is given by the equation

$$\left| \int_{t_R}^{t_p + t_{R,0}} C\mathrm{d}t \right| = C_0 t_p = \frac{n}{F_v} \tag{17}$$

Alternatively, the following equations give the maximum concentration:

$$\left| q(C_{Max}) - C_{Max}\frac{\partial q}{\partial C}_{C=C_{Max}} \right| = \frac{C_0 t_p}{F t_0} = \frac{n}{F t_0 F_v} \tag{18}$$

the combination of eqns. 15 and 18 give the retention time, t_R.

Eqns. 17 and 18 can be solved in closed form for a number of classical isotherms, such as the parabolic isotherm (see below), the Langmuir isotherm[31], the Freundlich isotherm or a two-term Langmuir isotherm[32]. Although it is probable that eqn. 18 can be solved for a number of other simple functional dependences, it cannot be so in the general case. Numerical solutions of eqn. 18 are easy to calculate, however.

The Langmuir isotherm is the most frequently used in liquid chromatography. It is given by

$$q = \frac{aC}{1 + bC} \tag{19}$$

In this case, eqn. 15 gives the rear profile[31]:

$$C = \frac{1}{b}\left[\sqrt{\frac{t_{R,0} - t_0}{t - t_p - t_0}} - 1\right] \tag{20}$$

and eqn. 17 gives the retention time[31]:

$$t_R = t_p + t_0 + (t_{R,0} - t_0)(1 - \sqrt{L_f})^2 \tag{21}$$

The Houghton[36] and the Haarhoff–Van der Linde[20] solutions are derived for the parabolic isotherm obtained by a two-term expansion of the Langmuir isotherm (eqn. 19):

$$q = aC(1 - bC) \tag{22}$$

We give here, for the sake of comparison, the solutions of eqns. 15 and 17 corresponding to this isotherm. The retention time of the band front is

$$t_R = t_{R,0} + t_p - 2(t_{R,0} - t_0)\sqrt{L_f} \tag{23}$$

and the equation for the continuous, diffuse profile which is eluted after the front shock is

$$C = \frac{1}{2b} \cdot \frac{t_{R,0} + t_p - t}{(t_{R,0} - t_0)} \tag{24}$$

Combining eqns. 23 and 24 gives the maximum concentration of the band, C_{Max}:

$$C_{Max} = \sqrt{L_f}/|b| \tag{25}$$

In these equations, t_p is the band width of the injection rectangular pulse, t_0 is the hold-up time, $t_{R,0}$ is the retention time of the compound at infinite dilution, *i.e.*, $t_0(1 + k'_0)$, and L_f is the loading factor, which is defined for a Langmuir isotherm as equal to the ratio of the amount injected to the monolayer capacity:

$$L_f = \frac{bn}{\varepsilon SLk'_0} \tag{26}$$

where n is the sample size in moles, S the column cross-sectional area and L the column length. The same definition applies to the parabolic isotherm which is used here as an approximation of the Langmuir isotherm and is not expected to be valid at high concentrations.

We note in passing that this profile is identical with the asymptotic solution of the ideal model for the Langmuir isotherm, which has been reported previously[32]. This result is expected as the asymptotic solution depends only on the origin slope and curvature of the isotherm.

Houghton solution

Originally, Houghton derived this solution on the assumption that the mass transfer kinetics are infinitely fast, but that the axial dispersion cannot be neglected[36]. However, in view of our previous discussion, the demonstration remains valid for mass

transfer kinetics which proceed at a finite but fast rate. The mass balance equation for the compound studied can be written as

$$u\frac{\partial C}{\partial z} + \left(1 + F\frac{dq}{dC}\right)\frac{\partial C}{\partial t} = D_a\frac{\partial C^2}{\partial z^2} \tag{27}$$

For the second-degree polynomial isotherm (eqn. 22), eqn. 27 becomes

$$\frac{\partial C}{\partial t} + \frac{\Lambda u C}{(1 + k'_0)(1 + \Lambda C)}\cdot\frac{\partial C}{\partial \xi} = \frac{D_a}{(1 + k'_0)(1 + \Lambda C)}\cdot\frac{\partial C^2}{\partial \xi^2} \tag{28}$$

with

$$\Lambda = -2b\frac{k'_0}{1 + k'_0} \tag{28a}$$

and

$$\xi = L\frac{t_{R,0} - t}{t_{R,0}} \tag{28b}$$

Eqn. 28 cannot be solved in closed form and a further simplification is necessary. Houghton proposed that the term ΛC in the denominators of the second term of the left- and right-hand sides of eqn. 28 be neglected, which gives

$$\frac{\partial C}{\partial t} + \frac{\Lambda u C}{(1 + k'_0)}\cdot\frac{\partial C}{\partial \xi} = \frac{D_a}{(1 + k'_0)}\cdot\frac{\partial C^2}{\partial \xi^2} \tag{28c}$$

It is important to note that, when this simplification is made, eqn. 28c is no longer a mass balance equation, *i.e.*, it no longer conserves mass. Using the Cole–Hopf transform, a solution of eqn. 28c can be derived. This solution, referred to later in this text as the Houghton equation, gives the elution profile of a pulse of finite width at the end of an infinitely long column[36]. Jaulmes and co-workers[37,38] simplified the Houghton equation for an impulse input (infinitely narrow pulse).

The Houghton solution for an infinitely narrow injection pulse can be written in dimensionless coordinates as follows, by using the values of Λ and ξ (eqns. 28a and 28b, respectively):

$$X = \left|\frac{\exp(-\tau^2/2)}{\sqrt{2\pi}[\coth m + \operatorname{erf}(\tau/\sqrt{2})]}\right| \tag{29}$$

where m is the dimensionless sample size, originally[36,37] given by

$$m = \frac{u^2\Lambda A}{2D_a S(1 + k'_0)} \tag{30a}$$

where A is the peak area, and which it is convenient to rewrite as

$$m = \frac{Lu}{2D_a}\left(\frac{k'_0}{1+k'_0}\right)^2 L_f \tag{30b}$$

τ is the dimensionless time, given by

$$\tau = \frac{k'_0 L}{(1+k'_0)\sqrt{D_a t}} \cdot \frac{t_{R,0}-t}{t_{R,0}-t_0} \tag{31}$$

and X is the dimensionless concentration, originally[37] given by

$$X = \left|\frac{\Lambda C}{2}\sqrt{\frac{u^2 t}{2D_a(1+k'_0)}}\right| \tag{32a}$$

but which it is more convenient to write as

$$X = |b|C\frac{k'_0}{1+k'_0}\sqrt{\frac{u^2 t}{2D_a(1+k'_0)}} \tag{32b}$$

Finally, Houghton also gave the solution of the ideal model, obtained as the limit of eqn. 29 when the apparent diffusion coefficient tends towards zero. The equation of the continuous rear part of the profile is

$$C = \frac{t_{R,0}}{2|b|t}\left(\frac{t_{R,0}+t_p-t}{t_{R,0}-t_0}\right) \tag{33}$$

This equation is different from the rigorous solution of the ideal model in the case of a parabolic isotherm, given in eqn. 24, and this shows that the Houghton equation cannot be correct (see below).

Haarhoff and Van der Linde solution

Haarhoff and Van der Linde derived equations for the band profiles of both a finite size sample pulse and an impulse (injection pulse with infinitely narrow width). They used the same assumptions as Houghton but they added one more. They decided to calculate the effect of dispersion on the band at $t = t_{R,0}$, arguing that the solute concentration at column outlet is significantly different from zero only during a period of time which is of the same order of magnitude as the standard deviation of the Gaussian peak observed for an infinitely small sample size and that the column length is assumed to be infinite (in practice, much longer than the HETP). Because of this new assumption, the two solutions are significantly different.

The elution band profile is given by the same eqn. 29, but as the apparent dispersion coefficient, D_a is equal to $Hu/2$, we can replace $Lu/2D_a$ in eqn. 30b by N, so that the dimensionless sample size becomes

$$m = N\left(\frac{k'_0}{1+k'_0}\right)^2 L_f \tag{34}$$

Similarly, in eqn. 31 we now have $D_a t = D_a t_{R,0} = Hut_{R,0}/2$, so this equation becomes

$$\tau = \sqrt{N}\frac{k'_0}{1 + k'_0}\cdot\frac{t - t_{R,0}}{t_{R,0} - t_0} \tag{35}$$

Finally, eqn. 32b can be written as

$$X = |b|C\frac{k'_0}{1 + k'_0}\sqrt{N} \tag{36}$$

The Haarhoff–Van der Linde equation is the combination of eqns. 29 and 34–36. The limit of this equation, when the column efficiency becomes infinite, is now identical with the rigorous eqn. 24. We also note for further reference that if we differentiate eqn. 29, to obtain the coordinates of the band maximum, we obtain the following result:

$$X_{Max} = \frac{|\tau_{Max}|}{2} \tag{37a}$$

Combination of eqns. 29, 35 and 37 permits the calculation of the exact retention time. Unfortunately, this cannot be solved in close form. However, combination of eqns. 35–37a gives a useful relationship:

$$k' = k'_0(1 - 2bC_{Max}) \tag{37b}$$

Comparison between the different solutions of the ideal and semi-ideal model

We have four different solutions available for predicting the elution profile of a compound at high concentration: the numerical solution[3,35], which can serve as a reference to compare with the solutions of the other three approaches, the Houghton and the Haarhoff–Van der Linde equations and the solution of the ideal model. We discuss first the advantages and drawback of the Houghton and Haarhoff–Van der Linde equations and compare them together. We then present a similar discussion for the analytical solution of the ideal model and compare it with the previous two solutions. Finally, we discuss the advantages and inconveniences of the numerical solution.

Haarhoff–Van der Linde and Houghton equations: influence of the first approximation, C is small. These two equations[20,36] are very similar and both make the same two basic assumptions in order to arrive at a closed form equation for the elution band profile: the sample size is small enough and the term AC can be neglected compared to unity, and the equilibrium isotherm can be replaced with its first two-term expansion. We discuss first the range of validity of these assumptions and their consequences.

As mentioned earlier, it is assumed in the derivation of both equations that the sample size is small and the term AC can be neglected compared with unity in the denominator of two terms of eqn. 28. Houghton[36] suggested that, in order to satisfy this assumption, the sample size should be such that the product $|AC_{Max}|$ should not exceed 0.05. This condition is equivalent to $|bC_{Max}k'_0/(1 + k'_0)| \leqslant 0.025$. This threshold usually corresponds to loading factors of *ca.* 0.001 or 0.1%. The equation

obtained by simplifying eqn. 28 and dropping the two $(1 + \Lambda C)$ terms is no longer mass conservative and is inaccurate at the first order [a correct first-order approximation would replace the terms $1/(1 + \Lambda C)$ by $(1 - \Lambda C)$, not by 1].

The fact that the Houghton equation is not mass conservative can cause a larger error. In the case of an upwardly convex isotherm, Λ is negative and the Houghton equation will predict an increasingly large mass loss when the sample size increases, as has been reported previously[39]. Conversely, for an upwardly concave isotherm, the Houghton equation leads to a mass gain which increases with increasing sample size. As the equation is incorrect at the first order, the mass loss or gain is proportional to the sample size at low values.

The Haarhoff–Van der Linde equation, which makes the same assumption, should suffer the same problem, but it does not because of the compensation which is introduced by calculating the axial dispersion at $t = t_{R,0}$. There is no mass loss or gain with this equation.

An exact equation for the band profile of a compound experiencing a parabolic isotherm has to be a rigorous solution of eqn. 28. There does not seem to be such a solution in closed form. An approximation has to be made, as was done by both Houghton and Haarhoff and Van der Linde. We suggest here another such approximation, which has the advantage of being more accurate than the Houghton equation and of not making the additional assumption made by Haarhoff and Van der Linde for the calculation of axial dispersion, although it results in a band profile equation which is identical with the latter.

Instead of dropping the term $1/(1 + \Lambda C)$ from eqn. 28 completely, we include it in the definition of Λ and D_a. Then, we replace C in these terms by the value derived from eqn. 24, *i.e.*, by the concentration obtained for an infinitely efficient column, which is $1 + \Lambda C = t/t_{R,0}$. This calculation gives an equation similar to the Houghton equation (eqn. 29). However, in eqns. 30a and 32a, D_a and Λ must be replaced, D_a by $D_a/(1 + \Lambda C)$, equal to $D_a t_{R,0}/t$, and Λ by $\Lambda/(1 + \Lambda C)$, equal to $\Lambda t_{R,0}/t$. Substituting these new parameters in the Houghton equation (eqns. 29–32) gives exactly the Haarhoff–Van der Linde equation (eqns. 29 and 34–36) and constitutes a simpler and more natural procedure for deriving it. This demonstration has the further advantage of explaining why the Haarhoff–Van der Linde equation conserves mass.

Our derivation gives an approximate solution of eqn. 28 which is much closer to the exact solution of eqn. 28 than the solution of eqn. 28c, which was derived by Houghton. Because of the $(1 + \Lambda C)^{-1}$ terms, eqn. 28 cannot be solved in closed form. Replacing these terms by a close approximation (derived from the solution of the ideal model) provides a much better approximate solution than dropping the terms entirely and, especially, eliminates the mass loss encountered with the Houghton equation.

In conclusion, although it is not a rigorous solution, the Haarhoff–Van der Linde equation is a much better approximation of the band profile than the Houghton equation. It is more accurate, it conserves mass and it can be used for any sample size, as long as the equilibrium isotherm is correctly approximated by a parabolic equation. Fig. 1 shows a comparison between the profiles predicted by the two equations, for sample sizes corresponding to loading factors of 0.01–0.2%, with a column efficiency of 12 500 theoretical plates. At very low column loadings, the two equations agree exactly. Significant differences appear for a loading factor of 0.1% and they increase rapidly with increasing sample size. Also, an increasing relative mass loss is observed,

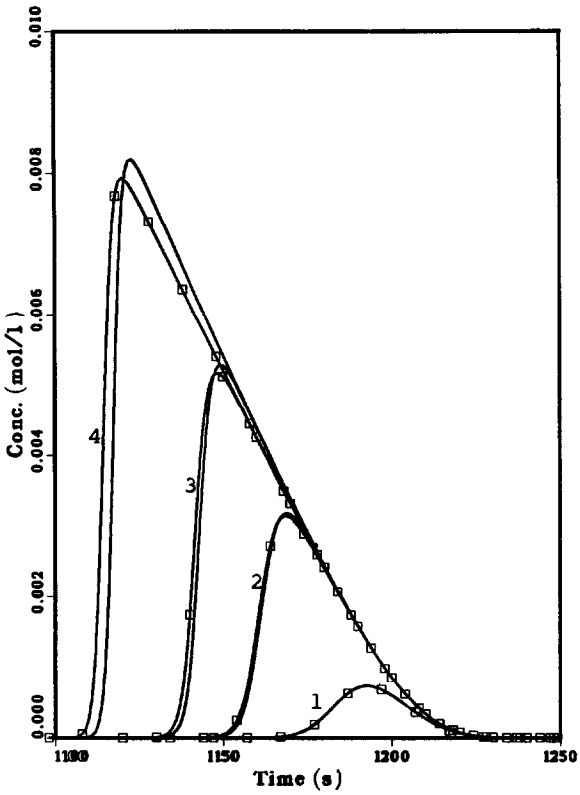

Fig. 1. Comparison between the band profiles predicted by the Houghton and Haarhoff–Van der Linde equations. Parabolic isotherm (eqn. 22), with $a = 20, b = 5$. Column length, 25 cm; phase ratio, 0.25; dead time, $t_0 = 200$ s; column efficiency, 12 500 theoretical plates. Loading factors: (1) 0.01%; (2) 0.05%; (3) 0.10%; (4) 0.20%. The Haarhoff–Van der Linde profiles are identified by squares. The masses lost by the Houghton profiles are (1) 0.2%, (2) 0.9%, (3) 1.5% and (4) 2.5%.

which is already 2.5% for a loading factor of 0.2%. Fig. 2 compares the band profiles obtained with the two equations, using a convex and a concave isotherm, with an equal absolute value for the second degree coefficient, b (see eqn. 22), and the same loading factor of 1% in both instances. The sign of the deviation between the two equations is reversed, and also the sign of the mass loss: with the upward convex isotherm the mass loss is 5.3% and with the downward convex isotherm the mass gain is 4.5%. It is obvious, however, that the difference has become larger than the experimental errors and one equation, the Houghton equation, has become unsuitable to account for band profiles.

Haarhoff–Van der Linde and Houghton equations: influence of the second approximation, a parabolic isotherm. The second major assumption made by Houghton[36] and by Haarhoff and Van der Linde[20] is that the isotherm is parabolic. We know that this has to be a simplification, but it is always possible to replace any isotherm by its first two-term expansion, at least in a certain concentration range. We have shown, however, that the band profile is extremely sensitive to small fluctuations of the isotherm[3]. This is why, in order to assess the value of our theoretical work on the

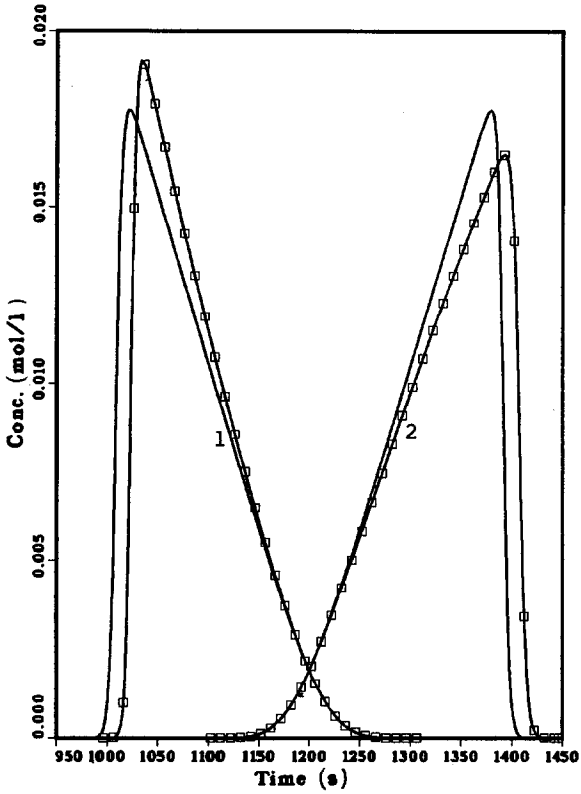

Fig. 2. Comparison between the band profiles predicted by the Houghton and Haarhoff–Van der Linde equations. Parabolic isotherms. Conditions as in Fig. 1, except loading factor, 1% in all instances. (1) Convex upward isotherm (eqn. 22, $b = 5$); (2) concave upward isotherm (eqn. 22, $b = -5$). The Houghton profiles are identified by squares. The masses lost by the Houghton profiles are (1) 5.3% and (2) −4.5%.

prediction of the band profiles of overloaded columns, we had to carry out accurate determinations of the equilibrium isotherms, and these measurements must be done on the very column on which the overloaded bands whose profiles are studied are eluted[40,41]. Hence, we may expect the replacement of the isotherm by its first two-term expansion to have some effect on the band profile even at low concentrations.

Haarhoff and Van der Linde[20] have discussed this problem. They concluded that for most isotherms used in practice, their equation should give accurate band profiles, as long as the following conditions is satisfied:

$$N_{th} = 16\left(\frac{t_{R,0}}{W_{th}}\right)^2 = \frac{4}{L_f}\left(\frac{t_{R,0}}{t_{R,0} - t_0}\right)^2 \geqslant 2000 \tag{38a}$$

or

$$L_f \leqslant 0.002\left(\frac{1 + k'_0}{k'_0}\right)^2 \tag{38b}$$

In eqn. 38a, W_{th} is the baseline band width of the band profile predicted by the ideal model for a parabolic isotherm (see eqn. 23).

Thus, after Haarhoff and Van der Linde, their equation should give satisfactory results with any isotherm, provided that the loading factor is less than about 0.2% or, from eqn. 25, $bC_{Max} \leqslant 0.05$. Increasing further the loading factor results in less and less accurate band profiles, not because of the approximation made in the derivation of the analytical solution (see above) but because of the progressive deviation between the quadratic isotherm equation (eqn. 22) and the true isotherm.

A practical procedure for checking the degree of agreement between the band profiles predicted by the Haarhoff–Van der Linde equation and the true profile starts by choosing a Langmuir isotherm. The elution band profiles are calculated for samples of increasingly large size, using the numerical solution of eqn. 12. These profiles are compared with the solutions of the Haarhoff–Van der Linde equation derived using the first two-term expansion of the same Langmuir isotherm. For a Langmuir isotherm, the true thermodynamic band width is given by the equation[31]

$$W_{th} = (2\sqrt{L_f} - L_f)(t_{R,0} - t_0) \tag{39}$$

whereas with a parabolic isotherm it is

$$W_{th} = 2\sqrt{L_f}(t_{R,0} - t_0) \tag{40}$$

The first band width is the product of multiplying the latter by $1 - \sqrt{L_f}/2$, a factor which becomes really significant when the loading factor exceeds 1%. The difference between the two values of the thermodynamic band width calculated with eqns. 39 and 40, for values of the loading factor of 1 and 10%, are 5% and 18%, respectively. Obviously, however, when the column efficiency is low, the band maximum concentration is smaller than predicted by the ideal model, and the concentration range sampled by the band during its elution is correspondingly narrower. Hence, the parabolic isotherm can be used to account for the elution band profiles of larger size samples with lower efficiency columns than with higher efficiency columns, the critical condition being that bC_{Max} is less than 0.05.

Haarhoff–Van der Linde and Houghton equations: conclusion. The last assumption made by Haarhoff and Van der Linde is that the band profile becomes Gaussian when the sample size becomes infinitely small, *i.e.*, under the conditions of linear chromatography. Therefore, the model cannot be used when the mass transfer kinetics are slow and the column efficiency for small size samples is lower than about 500 theoretical plates.

In conclusion, the Haarhoff–Van der Linde equation provides an excellent representation of the elution band profiles at low column loadings, and with most HPLC columns it should be used as a convenient model for values of the loading factor not exceeding 0.2% for ideal columns ($bC_{Max} \leqslant 0.05$ for real columns). This equation can be used with loading factors of up to 1% for ideal columns ($bC_{Max} \leqslant 0.1$ for real columns), which gives an error in the band width not exceeding 5%, except, however, for the low-efficiency columns which have to be used in affinity chromatography or with some other highly specific retention mechanisms. On the other hand, we have

regretfully come to the conclusion that the use of the Houghton equation should generally be avoided.

Ideal model and the Haarhoff–Van der Linde equation. Central to the ideal model is the assumption that the column efficiency is infinite. This constitutes its major drawback when the profiles that it predicts are compared with real profiles or with those predicted by other methods, such as the Haarhoff–Van der Linde equation. Obviously, in linear chromatography the results predicted by the ideal model are unrealistic, as the elution band profile would be identical with the injection profile, since there is no band broadening. On the other hand, when the loading factor increases, especially at high column efficiency, the results of the ideal model become closer and closer to the actual band profiles. With higher and higher column efficiency, with larger and larger sample sizes, the contribution of thermodynamics, *i.e.*, of the non-linear behavior of the equilibrium isotherm to the width of the band profile, becomes more and more important. This is the contribution for which the ideal model accounts.

In fact, the effective loading factor for a real column is given by eqn. 34. It turns out that the ideal model gives a realistic representation of the true band profile whenever the effective loading factor is greater than 35. Fig. 3 shows a comparison

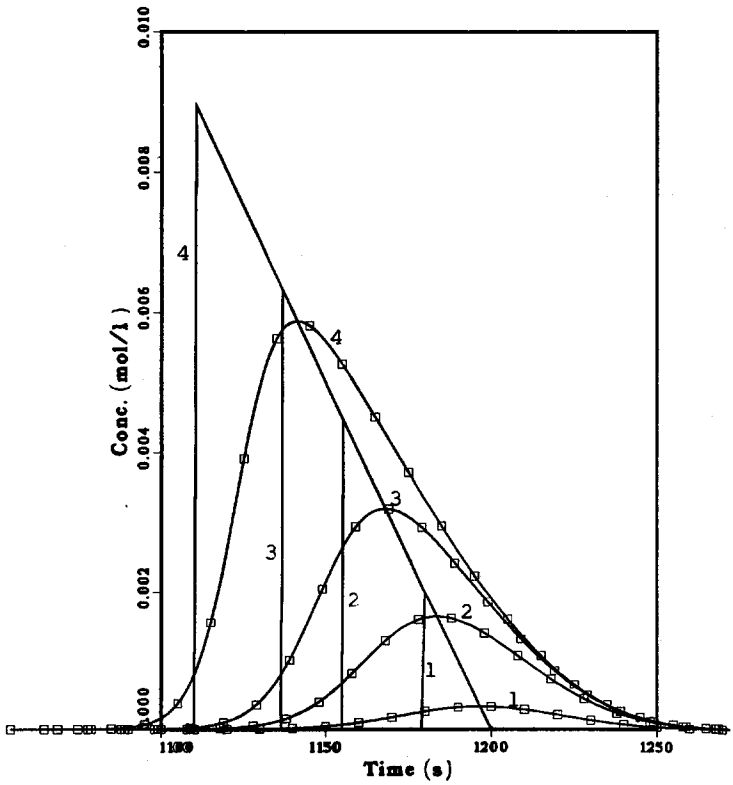

Fig. 3. Comparison between the band profiles predicted by the ideal model and the Haarhoff–Van der Linde equations. Parabolic isotherms, as for Fig. 1. Conditions as in Fig. 1, except column efficiency, 2500 plates ($m \leqslant 3.5$). Loading factors: 1, 0.01%; 2, 0.05%; 3, 0.1%; 4, 0.2%. The Haarhoff–Van der Linde profiles are identified by squares.

between the band profiles predicted by the ideal model and by the Haarhoff–Van der Linde equation, using in both instances a parabolic isotherm (note that the loading factor is calculated for the Langmuir isotherm having the same origin slope and curvature as the parabolic isotherm selected), for a column having 2500 theoretical plates. As expected, as the effective loading factor, m, is small (between 0.18 and 3.5), the agreement between the two models is poor, the Haarhoff–Van der Linde equation giving in this instance an excellent description of the true elution band profiles. Obviously, the ideal model cannot and should not be used in such instances.

Fig. 4, in contrast, shows a series of band profiles obtained with high column efficiencies and the same values of the loading factor as in Fig. 3. This time, the effective loading factor is $m = 35$ in all instances. The agreement between the two models is now excellent. It can only improve if the value of m exceeds 35. In Fig. 4, the retention time predicted by the ideal model is shorter by only 0.5% than the retention time predicted by the Haarhoff–Van der Linde equation, the band is 9% taller and it does not tail.

In order to assess better what in the systematic error made with the Haarhoff–Van der Linde equation comes from considering a parabolic isotherm and what is due

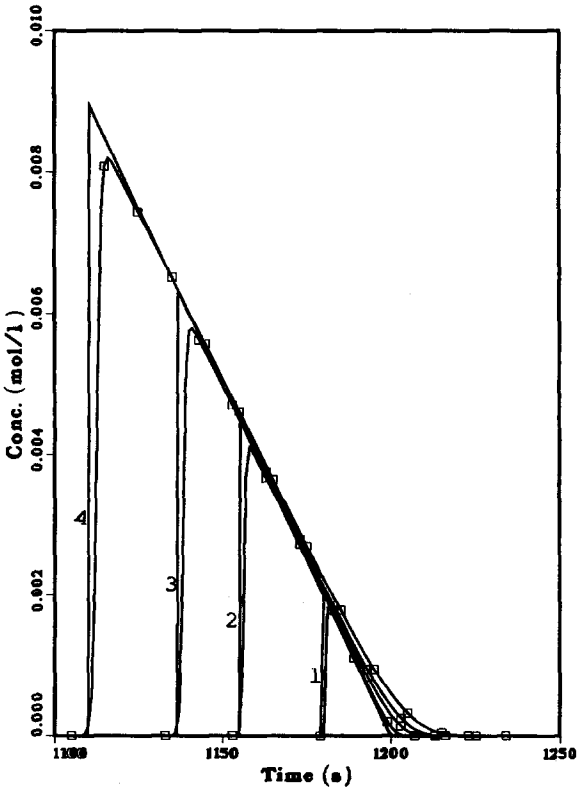

Fig. 4. Comparison between the band profiles predicted by the ideal model and the Haarhoff–Van der Linde equations. Parabolic isotherms, as for Fig. 1. Conditions as in Fig. 3, except column efficiency. Reduced sample size, $m = 35$. Loading factors and efficiency: (1) $L_f = 0.01\%$, $N = 500\,000$; (2) $L_f = 0.02\%$, $N = 100\,000$; (3) $L_f = 0.1\%$, $N = 50\,000$; (4) $L_f = 0.2\%$, $N = 25\,000$. The Haarhoff–Van der Linde profiles are identified by squares.

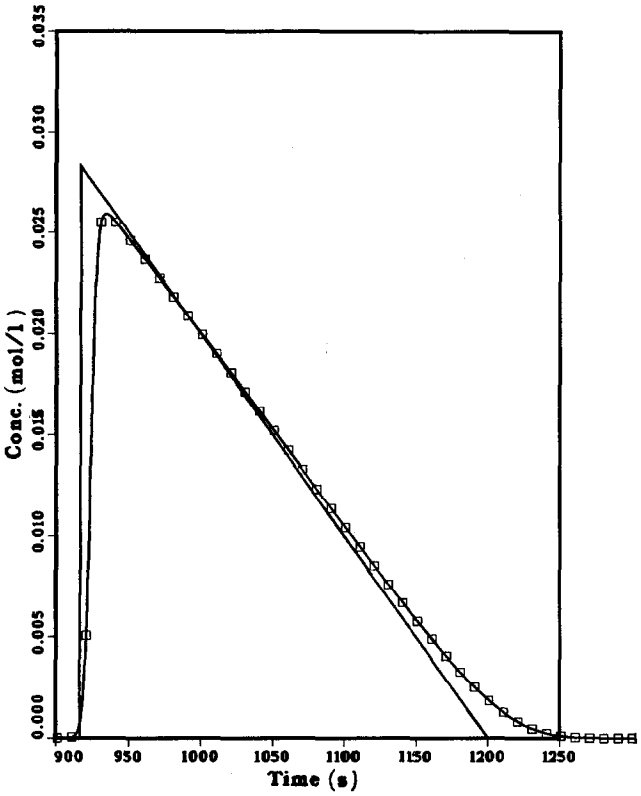

Fig. 5. Comparison between the band profiles predicted by the ideal model and the Haarhoff–Van der Linde equations. Parabolic isotherms, as for Fig. 1. Conditions as in Fig. 3, except loading factor, 2% (m = 35). The Haarhoff–Van der Linde profile is identified by squares.

to the assumptions made in the mathematical derivation, when considering the solute concentration C to be small, we have carried out some calculations in order to compare the band profiles predicted by the ideal model, with either a parabolic or a Langmuir isotherm, and by the Haarhoff–Van der Linde equation, using the same parabolic isotherm. The results are shown in Figs. 5 and 6.

Fig. 5 shows a comparison between the profile predicted by the two models for a parabolic isotherm, a column efficiency of 2500 theoretical plates (as for Fig. 3) and a loading factor L_f = 2%. The agreement between the two profiles, which now correspond to a reduced sample size m = 35, is very good.

Fig. 6 shows a comparison between the profile predicted by the ideal model for a Langmuir isotherm and the profile predicted by the Haarhoff–Van der Linde equation for the corresponding isotherm. All experimental conditions are the same as in Fig. 5. The Haarhoff–Van der Linde profile is, of course, the same for both Figs. 5 and 6. The agreement between the two profiles is much less satisfactory than in Fig. 5. The retention time of the ideal model profile is the same as that of the Haarhoff–Van der Linde profile, but the latter profile begins to elute much earlier, its height is much lower and the rear part of the two profiles intersect, instead of being tangential along

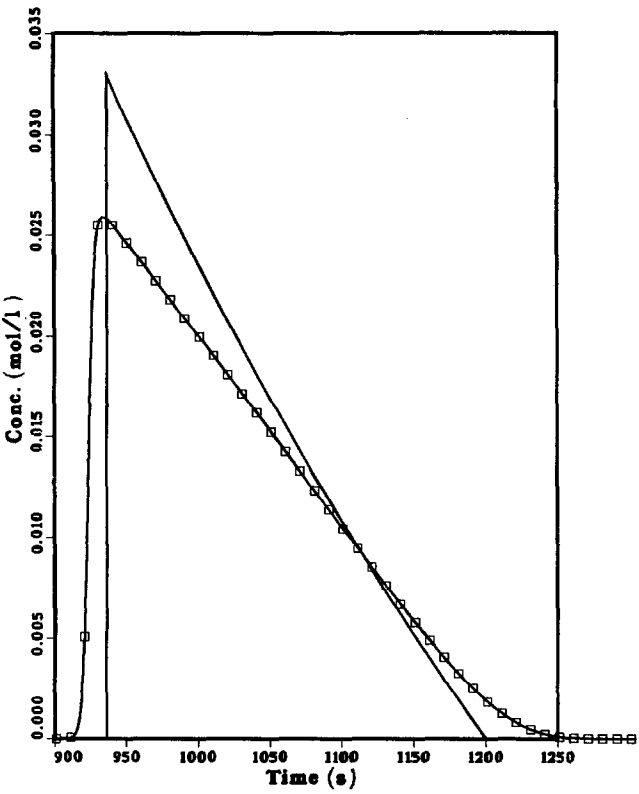

Fig. 6. Comparison between the band profiles predicted by the ideal model and the Haarhoff–Van der Linde equations. Parabolic isotherm as in Fig. 1 for the Haarhoff–Van der Linde equation, corresponding Langmuir isotherm for the ideal model. Conditions as in Fig. 5. The Haarhoff–Van der Linde profile is identified by squares.

a long arc. The comparison between Figs. 5 and 6 shows that the maximum sample size at which the Haarhoff–Van der Linde equation can be used depends very much on the extent of the deviation between the actual isotherm and its two-term expansion. The assumption of a parabolic isotherm is the major limit to the validity of the Haarhoff–Van der Linde equation at large sample sizes.

Ideal model and the Houghton equation. Although we have shown above that the Houghton equation is not as good an approximate solution as the Haarhoff–Van der Linde equation, we carried out for it a similar comparison to that in the previous section between the results of the ideal model and those of the Haarhoff–Van der Linde equation.

Fig. 7 compares the elution band profiles obtained with the ideal model and with the Houghton equation for a compound with a parabolic isotherm and a 1% loading factor in both instances, and with a column efficiency of 5000 theoretical plates for the Houghton equation. There is a poor agreement between the two profiles. The mass loss experienced is 6.75%. This confirms our earlier conclusion that the Houghton equation cannot be used to account for elution band profiles at high loading factors.

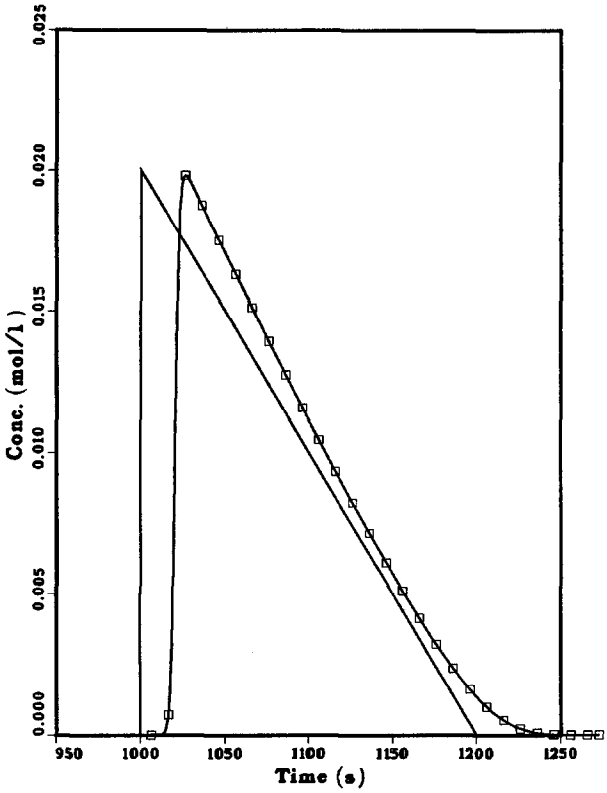

Fig. 7. Comparison between the band profiles predicted by the ideal model and the Houghton equations. Parabolic isotherms, as for Fig. 1. Conditions as in Fig. 1, except loading factor, L_f = 1%, and column efficiency, 5000 plates (m = 35). The Houghton profile is identified by squares. The mass loss is 6.75%.

not only because of the parabolic isotherm assumption, but also because of the approximation made in the derivation of this equation and the resulting mass loss or gain. The comparison between Figs. 5 and 7 illustrates this problem.

Fig. 8 shows a comparison between the band profile predicted by the ideal model for a Langmuir isotherm and by the Houghton equation for the two-term expansion of this Langmuir isotherm. The agreement is now almost satisfactory, not because of the validity of the Houghton equation, but because of some error compensation. The loss of the AC term partially compensates for the change in the isotherm. It is certain, however, that a least-squares adjustment of the Houghton equation on experimental data will, in most instances, lead to values of the experimental parameters which have little or no physical meaning.

Haarhoff–Van der Linde equation and the dimensionless band profile plot. We have shown previously[31] that the band profiles obtained for increasing sample sizes of a given compound under constant experimental conditions can be scaled to a dimensionless form. This result was derived from theoretical considerations regarding the band profile obtained with the ideal model, assuming a Langmuir equilibrium isotherm.

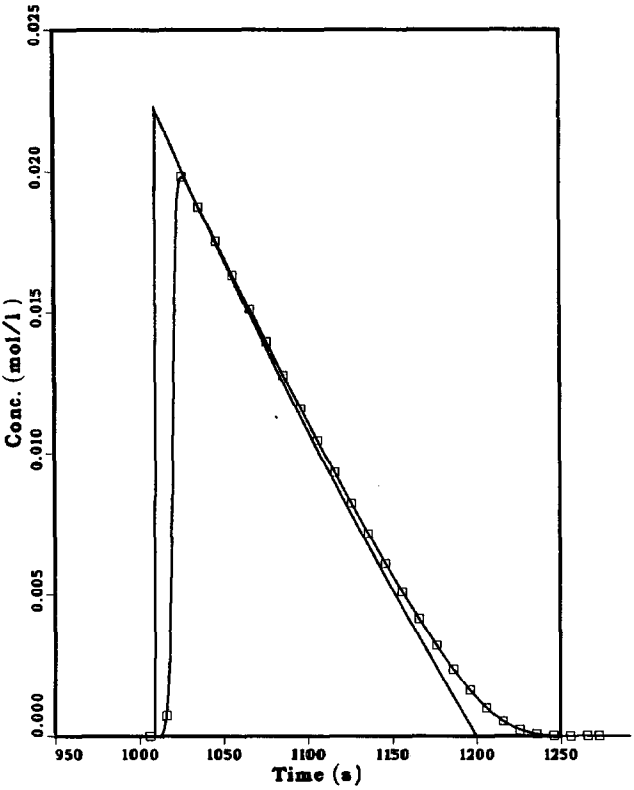

Fig. 8. Comparison between the band profiles predicted by the ideal model and the Houghton equations. Parabolic isotherm for the Houghton equation. Langmuir isotherm for the ideal model. Conditions as in Fig. 7. The Houghton profile is identified by squares.

With the ideal model, it is easy to show that a normalized dimensionless plot can be obtained by using $(t - t_0)/(t_{R,0} - t_0)$ as a reduced time coordinate and bC as a reduced concentration coordinate[31]. The profiles predicted by the Langmuir isotherm depend only on the loading factor, L_f, the ratio of the sample size to the column saturation capacity. This system of reduced parameters will be called the "ideal reduced coordinate system". We have shown that the degree of agreement between reduced plots of data obtained with real columns in the "ideal reduced coordinate system" is good only if the different columns have the same efficiency[31].

Similarly, eqns. 34–36 show that, for a real column with a finite efficiency and if the equilibrium isotherm is parabolic, a dimensionless plot can be obtained by using $\tau = \sqrt{N}k'_0(1 + k'_0)[(t - t_{R,0})/(t_{R,0} - t_0)]$ (see eqn. 35) as reduced time and $X = |b|C[k'_0/(1 + k'_0)]\sqrt{N}$ (see eqn. 36) as reduced concentration. The reduced sample size, which is the only parameter on which the normalized profiles depend, is $m = N[k'_0/(1 + k'_0)]^2 L_f$ (eqn. 34). This system of reduced parameters will be called the "Haarhoff–Van der Linde reduced coordinate system". We note that the reduced parameters depend on the column efficiency, N. We had already shown that the degree

of agreement between the solution of the ideal model and the numerical solution for a real column depends on the column efficiency and on the loading factor[31]. A correction can be derived which combines, through the variance additivity rule[20,42], the thermodynamic band width predicted exactly by the ideal model solution and the kinetic band width obtained from the efficiency of the band at infinite dilution[31,43].

This discussion provides a theoretical explanation to results which, previously, were merely qualitative. Eqn. 34, for example, explains why, and to what extent, an efficient column appears to be more overloaded by a given sample size than a less efficient column.

These results have such an important practical value that it is worthwhile investigating in detail now what their range of validity is. We note that Poppe and Kraak[44] and Eble *et al.*[45] have presented experimental results in a format that is compatible with the reduced plot just outlined (see next section).

Fig. 9 shows, in the Haarhoff–Van der Linde reduced coordinate system, a series of seven normalized band profiles corresponding to as many sets of different

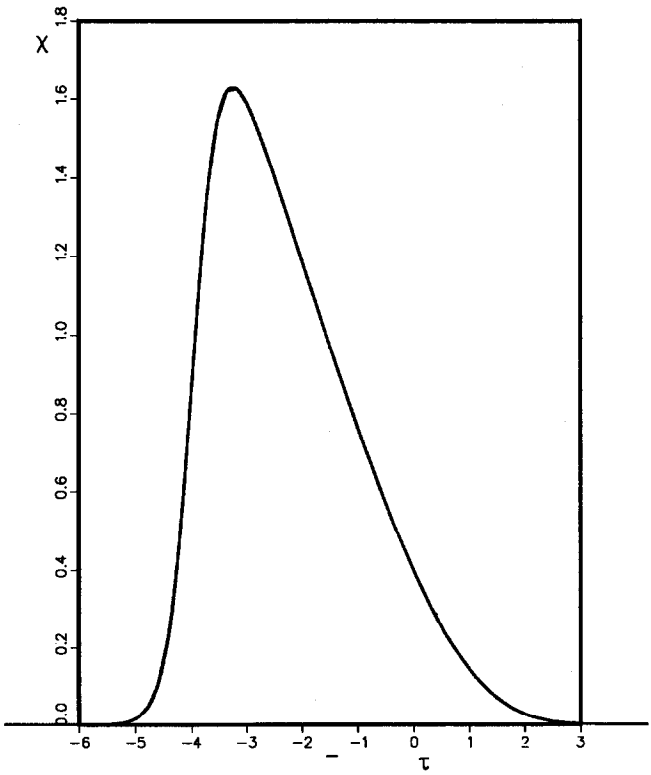

Fig. 9. Plot of seven superimposed band profiles predicted by the Haarhoff–Van der Linde equation, in the Haarhoff–Van der Linde reduced coordinate system (see text). Plot of reduced concentration (X, eqn. 36) *versus* reduced time (τ, eqn. 35). (1) N = 10 000, k'_0 = 1, b = 2, F_v = 1 ml/min; (2) same as (1), except N = 5000; (3) same as (1), except N = 1000 plates; (4) same as (2), except b = 5; (5) same as (2), except F_v = 5 ml/min; (6) same as (2), except k'_0 = 5; (7) same as (2), except k'_0 = 25. The loading factor is adjusted so that all conditions correspond to the same value of m = 5.

experimental conditions, all of them giving the same value of the normalized loading factor, *i.e.*, the reduced sample size, m. The curves cannot be distinguished. Fig. 10 shows a series of normalized band profiles corresponding to increasing values of the reduced loading factor, from 1 to 30. The result is very similar to that reported earlier, and corresponding to Langmuir isotherms[31]. It demonstrates the principle and the practical value of the band profile reduced plot.

Figs. 11 and 12 present the converse case. They exhibit band profiles calculated with a Langmuir isotherm and plotted in the Haarhoff–Van der Linde reduced coordinate system. The four profiles presented in each figure correspond to various experimental conditions giving the same value of the reduced sample size, m, of 3.5 for Fig. 11 and 35 for Fig. 12. We have shown in Fig. 9 that when the isotherm is parabolic all band profiles corresponding to the same value of the reduced sample size give the same plot in the Haarhoff–Van der Linde reduced coordinate system. Fig. 11 shows that for a reduced sample size of 3.5 the parabolic isotherm is already a poor representation of the Langmuir isotherm. The deviation is especially large for the profile corresponding to the less efficient column, but it should be emphasized that this profile corresponds also to the largest sample size (see eqn. 34). The scatter of the different plots and their deviations from the normalized Haarhoff–Van der Linde profile (see Fig. 10) increases as expected when m is increased from 3.5 (Fig. 11) to 35

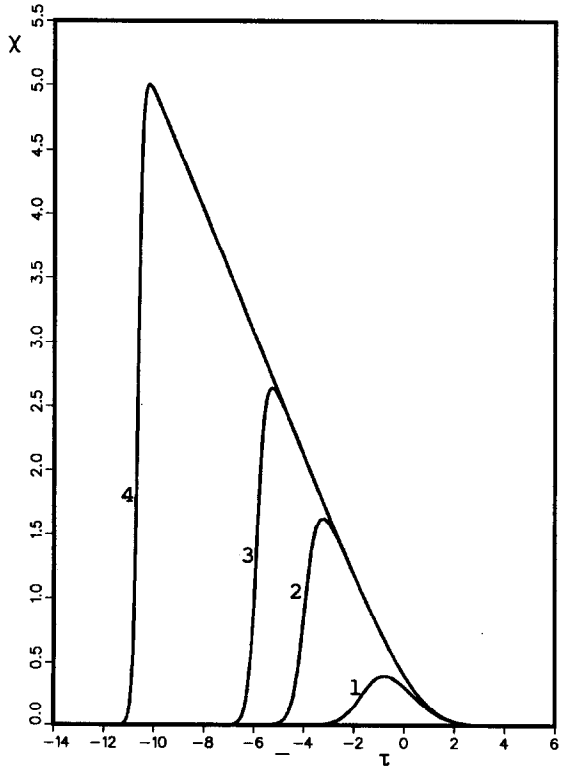

Fig. 10. Plot of band profiles predicted by the Haarhoff–Van der Linde equation, using the Haarhoff–Van der Linde reduced coordinate system (see text). Plot of reduced concentration (X, eqn. 36) *versus* reduced time (τ, eqn. 35). Influence of sample size. Reduced sample size, m: (1) 1; (2) 5; (3) 10; (4) 30.

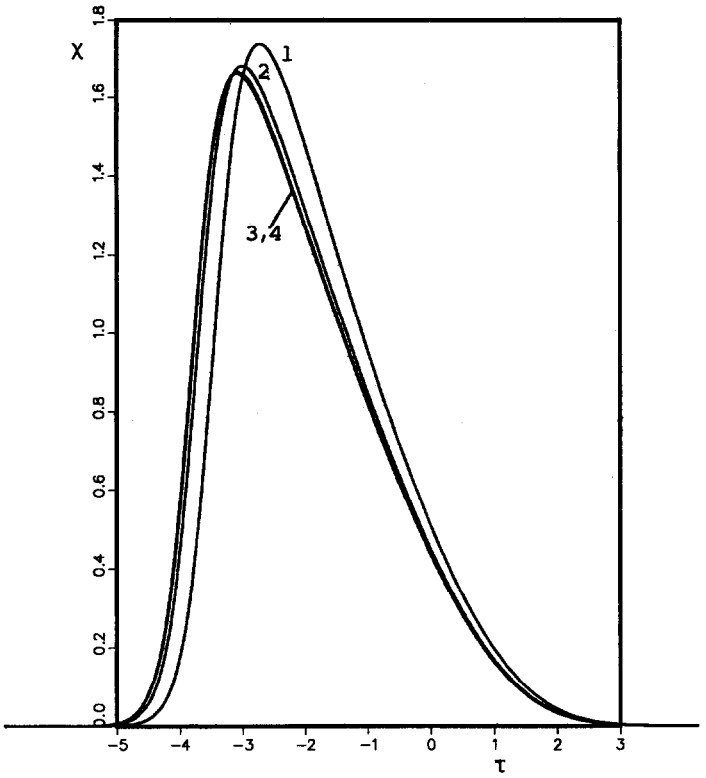

Fig. 11. Comparison between band profiles predicted by the numerical solution of the semi-ideal model, using the Langmuir isotherm, and plotted in the Haarhoff–Van der Linde reduced coordinate system (see text). Plot of reduced concentration (X, eqn. 36) *versus* reduced time (τ, eqn. 35). (1) $N = 1000, k'_0 = 1, b = 2, F_v = 1$ ml/min; (2) same as (1), except $N = 5000$; (3) same as (1), except $N = 10\,000$; (4) same as (2), except $k'_0 = 5$. The loading factors are chosen so that the reduced sample size $m = 3.5$.

(Fig. 12). These figures show that, if the isotherm is not parabolic but is Langmuirian, the Haarhoff–Van der Linde normalized plot is not applicable, and we must use the ideal reduced coordinate system, at fixed column efficiency[31].

Fig. 13 shows a plot of two band profiles in the ideal reduced coordinate system. These bands are both solutions of the ideal model, one using a parabolic isotherm and the other a Langmuir isotherm. The two profiles are tangential at the point ($t = t_{R,0}$, $C = 0$). The band profiles are nearly identical for a loading factor of 0.2% and remain very close for a loading factor of 1%. Above the latter value, the difference between them increases rapidly. This confirms that the practical maximum limit of validity of the Haarhoff–Van der Linde equation is for a loading factor of *ca.* 1% for ideal columns ($bC_{Max} \leqslant 0.1$ for real columns).

EMPIRICAL SOLUTIONS

Poppe and Kraak[44] have shown that the apparent plate number of a chromatographic band, N_{app}, is related to the sample size injected by the following equation:

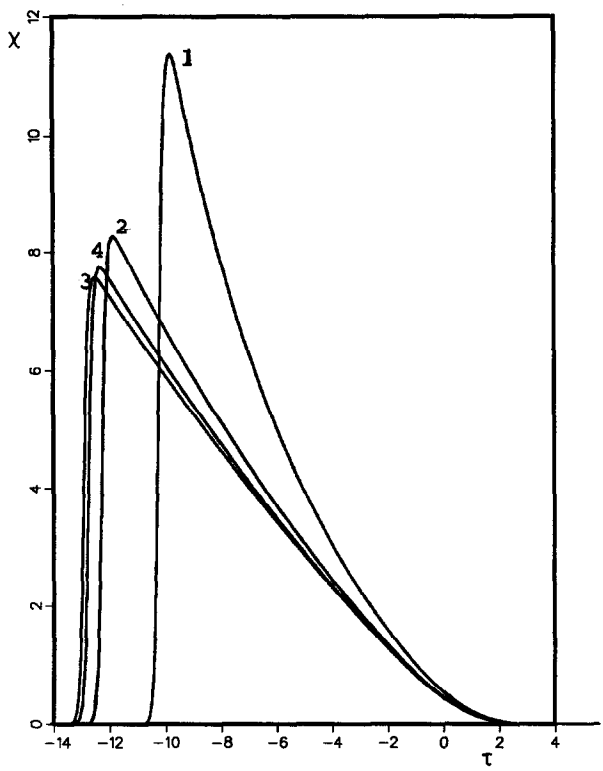

Fig. 12. Same as Fig. 11, except the loading factors are adjusted so that $m = 35$.

$$N_{app} = N f(m) \tag{41}$$

where N is the limit efficiency for a sample of infinitely small size and m has the same definition as in eqn. 34 above. A similar relationship was also given by Knox and Pyper[42]. This result has been used recently by Eble *et al.*[45,46]. Eqn. 41 derives directly from the Haarhoff–Van der Linde equation and from the fact that the profiles can be scaled (see above, Figs. 9 and 10). In fact, Fig. 4 in ref. 20 shows the same plot of the variation of the column apparent efficiency with m as Fig. 9 in ref. 44 and Fig. 5 in ref. 45.

Similarly, Eble *et al.*[45] have suggested that the apparent column capacity factor depends on the sample size through the equation

$$k' = k'_0 \, g\left(\sqrt{N}\frac{k'_0}{1 + k'_0}L_f\right) \tag{42}$$

where $g(\ )$ is a functional dependence. Fig. 4 in ref. 20 shows a plot of the variation of the apparent retention with m which is equivalent to Fig. 8 in ref. 44 and Fig. 6 in ref. 45. On the other hand, it results from eqn. 37 that the functional dependence of the retention time (*i.e.*, k') is

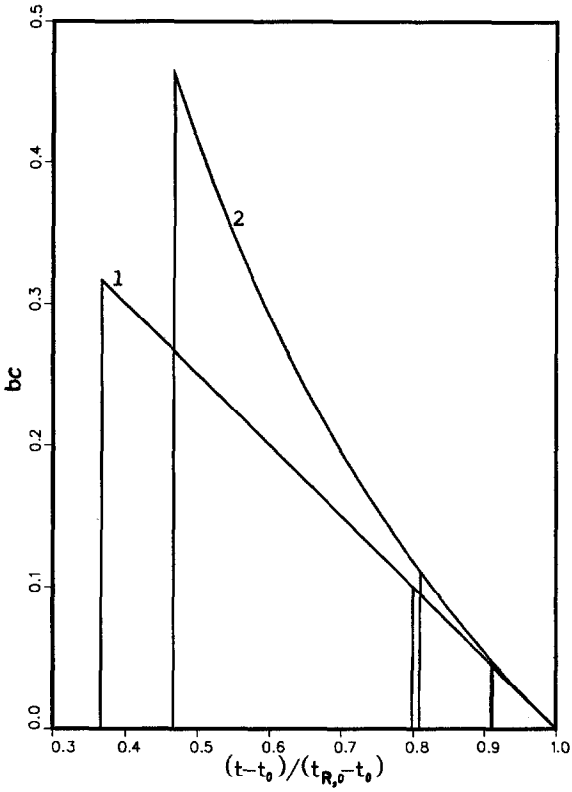

Fig. 13. Comparison between two band profiles calculated with the ideal model, using two different equilibrium isotherms. The plots are made in the ideal reduced coordinate system (see text). (1) Parabolic isotherm; (2) Langmuir isotherm.

$$\tau_{Max} = f(m) \tag{43a}$$

or

$$\sqrt{N}\frac{k'_0}{1+k'_0}\left(1-\frac{k'}{k'_0}\right) = f\left[N\left(\frac{k'_0}{1+k'_0}\right)^2 L_f\right] \tag{43b}$$

Eqn. 42 is not equivalent to eqn. 43b and is an incorrect oversimplification.

Eqns. 41 and 43 are valid only as far as the Haarhoff–Van der Linde equation is valid, that is, as we have shown above, as long as the loading factor does not exceed *ca.* 1%. Accordingly, the experimental results obtained by Eble *et al.* (Figs. 6–24 in ref. 46) are a convincing verification of the Haarhoff–Van der Linde equation. As explained in the previous discussions, the deviations from a universal plot which are observed at large sample sizes are explained by the incorrect assumption made by Haarhoff and Van der Linde of a parabolic isotherm.

Semi-empirical relationships such are those derived subsequently by Eble *et al.*[45]

used empirical parameters to force adjustment of experimental data on the universal plot. As the basic origin of the deviation observed, *i.e.*, the implicit assumption of a parabolic isotherm, was not understood, the approach has had only limited success.

As we have shown above, when the sample sizes used in preparative liquid chromatography correspond to values of the loading factor not exceeding 1% for ideal columns ($bC_{Max} \leq 0.1$ for real columns), the Haarhoff–Van der Linde equation and the corresponding dimensionless plot give successful predictions of the entire band profiles and of their sample size dependence. Then plots of N or k' *versus* complex functions of experimental parameters are of dubious practical interest as they give much less information. At higher values of the loading factors the only correct predictions can be obtained either with the solution of the ideal model, with a correction for finite efficiency[31,43] or through the calculation of numerical solutions.

CORRECTION OF THE ANALYTICAL SOLUTION OF THE IDEAL MODEL

There is no exact solution available for eqn. 12 at high concentration. The influence of a finite column efficiency on the band profile cannot be accounted for properly. In other words, we are in a situation comparable to that at low concentrations, where the Haarhoff–Van der Linde equation assumes a simplified isotherm to account for the onset of the influence of the non-linear thermodynamic behavior on a band profile which is still essentially controlled by the kinetics of mass transfer. We would like to account for the influence of the finite column efficiency on a band profile which is essentially controlled by the non-linear behavior of the isotherm, for which the ideal model accounts perfectly.

Although there is no rigorous solution to this problem, it can be handled approximately, by using a result classical in linear chromatography and extending it to non-linear chromatography. The original idea was presented by Haarhoff and Van der Linde[20] and by Knox and Pyper[42] and a more rigorous treatment was derived later[31]. We assume that the observed column height equivalent to a theoretical plate (HETP), $H_{app} = L/N_{app}$, is the sum of two independent contributions:

$$H_{app} = H + H_{th} \tag{44}$$

where H and H_{th} represent the kinetic and thermodynamic contributions to the HETP, respectively. There is no real theoretical basis to this assumption, which stems from the additivity of the independent contributions to the band variance in linear chromatography[47].

The first contribution, H, is equal to the HETP determined under linear conditions, assuming that the diffusion coefficients are independent of the solute concentration, which is valid in the concentration range used in preparative chromatography, for compounds of low or moderate molecular weight, and that the retention kinetics are fast. It accounts for the effect of the finite rate of mass transfer on the band width. The second contribution, H_{th}, results from the non-linear behavior of the isotherm and can be derived from our previous results on the ideal model, which account correctly for this effect, but for this effect only.

Eqn. 44 is equivalent to

$$N_{app} = \frac{NN_{th}}{N + N_{th}} \tag{45}$$

where N_{app}, N and N_{th} are the apparent plate number for a certain value of the loading factor, the plate number at infinite dilution for the same compound and the plate number resulting from the width of the profile as predicted by the ideal model, respectively.

This procedure has been used in the case of a Langmuir equation to calculate the band width and the apparent column efficiency[31]. It was found to give results in good agreement with those of the numerical calculations and with the experimental data previously acquired[43].

CONCLUSION

As we have mentioned in the previous section, the work by Eble *et al.*[46] provides a detailed verification of the validity of the Haarhoff–Van der Linde equation at low values of the column loading factor. An excellent agreement between the band profiles predicted by the ideal model and the profiles recorded for large samples of pure compounds has been reported under a variety of experimental conditions[43,48]. The only common characteristic of these experiments was that in most cases the reduced sample size, m, was larger than 35. A correction procedure which accounts for the band broadening due to finite column efficiency kinetics has been described[31,42]. The results were very satisfactory[43].

These experimental results confirm our conclusion that the use of the Houghton equation should be avoided, that the Haarhoff–Van der Linde equation gives excellent results for the prediction of band profiles at low loading factors ($L_f \leq 0.2\%$ for ideal columns or $bC_{Max} \leqslant 0.05$ for real columns), which become progressively less good with increasing loading factors. It should not be used with loading factors much in excess of *ca.* 1% for ideal columns ($bC_{Max} \leqslant 0.1$ for real columns). The ideal model give excellent results at high loading factors with values of m exceeding *ca.* 35, which, depending on the column efficiency and the retention, corresponds to values of the loading factor between 0.5% (very efficient columns, *e.g.*, $N = 10\,000$ plates and $k'_0 = 3$) and 3.3% (*e.g.*, $N = 1500$ plates and $k'_0 = 3$). In either instance, the use of the corresponding reduced coordinate system permits easy comparisons and predictions of the band profiles and of the effects of changes in the experimental conditions on these profiles and their sample size dependence.

If both analytical solutions fail, numerical solutions can be used, as discussed in the next section.

NUMERICAL SOLUTIONS OF THE SEMI-IDEAL MODEL FOR A SINGLE COMPOUND AND ANY ISOTHERM

We have shown above that the analytical solution derived by Haarhoff and Van der Linde[20] is valid for values of the loading factor such that $bC_{Max} \leqslant 0.05$. On the

other hand, we have also shown that the ideal model is valid when the reduced loading factor exceeds 35, which in most instances (*i.e.*, with columns having several thousand theoretical plates and values of k'_0 in excess of 2) corresponds to loading factor of several percent ($k'_0 = 2$, $N = 2500$ give $m = 35$ for $L_f = 3\%$). In the intermediate range of sample sizes, there is no satisfactory solution, although the band width of the profile at any fractional band height can be approximated, using the procedure suggested by Knox and Pyper[42].

As there is no analytical solution available, we have to resort to numerical calculations. Two approaches are available: the semi-ideal model, which can be used only when the limit efficiency of the column at infinite dilution of the sample exceeds *ca.* 500 theoretical plates, and the kinetic models, which are valid in the whole range of values of the rate constants. We discuss only the former approach, as this work deals with equilibrium and semi-equilibrium models. Kinetic models are discussed in a separate paper[1].

Numerical solutions

In the semi-ideal model, the mass transfer kinetics are handled in the same way as by Van Deemter *et al.*[14] and by Haarhoff and Van der Linde[20]. The axial dispersion coefficient, D, in the mass balance equation is replaced by an apparent dispersion coefficient, $D_a = Hu/2$, which combines all the effects which, in linear chromatography, are traditionally lumped in the column HETP. The system of the mass balance equation (eqn. 1) and the kinetic equation (eqn. 4) is therefore replaced by eqn. 12. This equation is an excellent approximation of the system of partial differential equations in chromatography whenever the mass transfer kinetics are fast enough and at very low sample sizes the band profile tends towards a Gaussian profile.

The great advantage of this approach is that we do not need any detailed information regarding the mass transfer kinetics and their dependence on the solute concentration. Such information is usually difficult to collect and requires long, complicated experiments which provide only indirect determinations. With the semi-equilibrium model, we need to know the column efficiency at infinite dilution, the sample size and the equilibrium isotherm between the two phases, which is also needed with the kinetic models. The numerical solutions can accommodate any isotherm of physical significance and require no simplification.

Numerical solutions, however, do create truncation errors, because of the necessary use of finite values of space and time increments in the integration. These errors must be minimized or controlled. The classical method of finite differences lends itself to a straightforward application in the present instance. Two approaches are available. They have been discussed in detail in several previous publications[35,49,50], so we present here only a brief review of the numerical analysis problems.

Characteristic procedure. In this approach[3,51], we neglect the right-hand side of eqn. 12, *i.e.*, we write a program as if we wanted to calculate solutions of the ideal model (eqn. 14). We calculate the concentration at each point of a grid ($nh, j\tau$). We replace each differential by a finite difference, calculated for small but finite increments of the variables, space (h) and time (τ), respectively. Various finite difference schemes can be used, each introducing different truncation errors. For example, we may write[3]

$$\frac{C_{n+1}^{j} - C_{n}^{j}}{h} + \frac{1}{u} \cdot \frac{C_{n}^{j} + Fq_{n}^{j} - C_{n}^{j-1} - Fq_{n}^{j-1}}{\tau} = 0 \tag{46a}$$

which can be solved for C_{n+1}^{j}:

$$C_{n+1}^{j} = C_{n}^{j} + \frac{h}{u\tau}(C_{n}^{j} + Fq_{n}^{j} - C_{n}^{j-1} - Fq_{n}^{j-1}) \tag{46b}$$

The concentration at any point $C(n + 1,j)$ of the grid can be calculated, knowing the concentrations at the points (n,j) and $(n,j-1)$.

This procedure creates an error, because the increments must remain finite. It can be shown that the error is equivalent to the addition of a dispersion term to the right-hand side of eqn. 14[49,50]. Therefore, the procedure gives solutions of eqn. 12. If the space increment, h, is equal to the column HETP (*i.e.*, to H) and the time increment is equal to $2H(1 + k'_0)/u$, the truncation error in linear chromatography is exactly equal to $D_a\partial^2 C/\partial z^2$, where $D_a = Hu/2$. Therefore, the elution band profile of a column having an HETP equal to H (eqn. 12) is simulated[49,50].

Lax–Wendroff procedure. In this procedure, we write a program to calculate directly the solutions of eqn. 12, not those of eqn. 14, as in the previous section. The same error calculation method (*i.e.*, replacement in the finite difference equation of the value of the concentration at each point of the grid by its first three-term expansion) shows that it is possible to eliminate the excess diffusion which could arise from the truncation errors by a proper choice of the differences, *i.e.*, by using the numerical scheme described by Lax and Wendroff (see ref. 35). In linear chromatography, we obtain the following equation:

$$\frac{C_{n}^{j+1} - C_{n}^{j}}{\tau} + u_z \frac{C_{n+1}^{j} - C_{n-1}^{j}}{2h} = \left(\frac{\tau u_z^2}{2} + \frac{D_a}{1 + k'_0}\right)\frac{C_{n+1}^{j} - 2C_{n}^{j} + C_{n-1}^{j}}{h^2} \tag{46c}$$

where $u_z = u/(1 + k'_0)$. The extra-term, $\tau u_z^2/2$, added to the diffusion coefficient term, is introduced to compensate for the truncation error.

This procedure, however, suffers from two major drawbacks. First, the method used for the cancellation of the errors, which permits a correct simulation of the diffusion term in the right-hand side of eqn. 12, is exact only in linear chromatography, where the result is the same as the result of the calculations made using eqn. 46b. In non-linear chromatography an error appears. At moderate values of the loading factor this error is a small time shift. At higher loading factors, the error is difficult to estimate. Second, the choice of the values of the space and time increments must be made in very narrow ranges, in order to avoid numerical instabilities, resulting in unacceptable profiles. For these reasons, we prefer the former approach.

Comparison between the analytical solutions of the semi-ideal models and the numerical solutions of the semi-ideal model

We compare here the results obtained by the numerical solution of eqn. 12 and the results given by the Haarhoff–Van der Linde equation. This comparison completes

that in the previous section between the profiles predicted by this equation and by the analytical solution of the ideal model.

Fig. 14 compares the band profiles predicted by the Haarhoff–Van der Linde equation and by the numerical solution, both using a parabolic isotherm, for loading factors between 0.01 and 0.2% and a column efficiency of 2500 theoretical plates. In all four cases, the agreement between the two profiles corresponding to the same loading factor is excellent. Fig. 15 shows the same comparison, except that a Langmuir isotherm is used for the calculation of the numerical solutions, and the two-term expansion of this Langmuir isotherm for the calculations of the Haarhoff–Van der Linde equation. Although the agreement between the two profiles corresponding to a given loading factor is still very good, some significant difference begins to appear at the highest column loading. This result confirms, nevertheless, that the Haarhoff–Van der Linde equation is an excellent approximation of the band profile at low loading factors.

Fig. 16 compares the profiles predicted by the Haarhoff–Van der Linde equation and the numerical solution, both for a parabolic isotherm and for a loading factor of

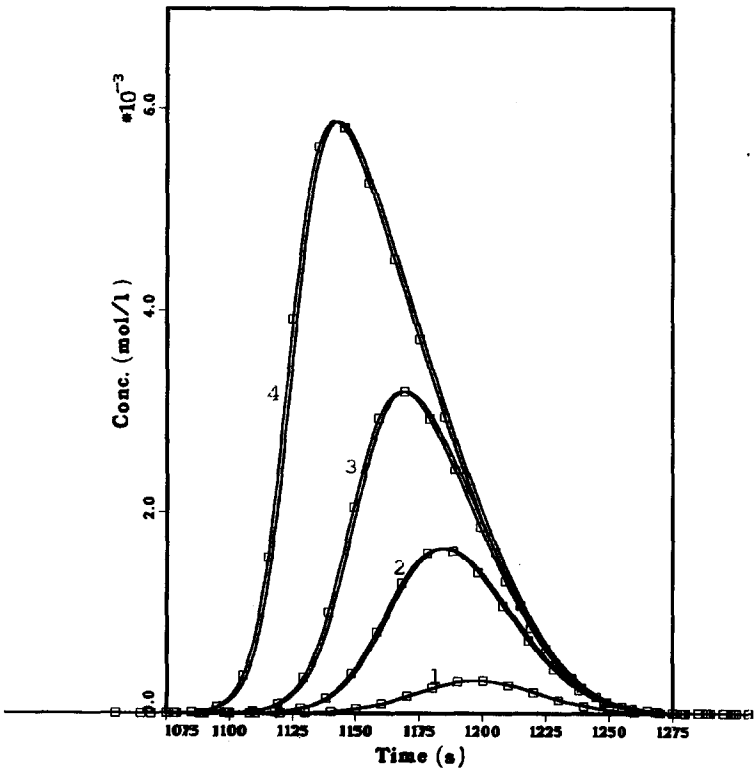

Fig. 14. Comparison between the band profiles predicted by the Haarhoff–Van der Linde equation and calculated by the numerical solution of the semi-ideal model. Parabolic isotherms, as for Fig. 1. Conditions as in Fig. 1, except column efficiency, 2500 plates. Loading factors: (1) 0.01%; (2) 0.02%; (3) 0.1%; (4) 0.2%. The Haarhoff–Van der Linde profiles are identified by squares.

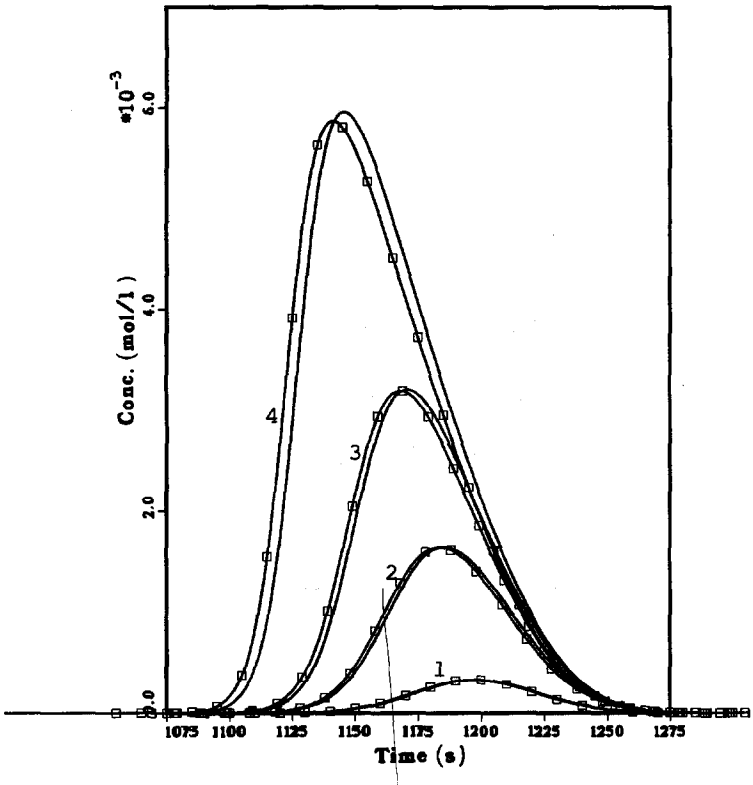

Fig. 15. Comparison between the band profiles predicted by the Haarhoff–Van der Linde equation and calculated by the numerical solution of the semi-ideal model. Parabolic isotherm as for Fig. 1 for the Haarhoff–Van der Linde equation, Langmuir isotherm for the numerical solution. Conditions as in Fig. 14. Loading factors: (1) 0.01%; (2) 0.02%; (3) 0.1%; (4) 0.2%. The Haarhoff–Van der Linde profiles are identified by squares.

0.2%, with increasing column efficiency. The agreement is excellent in all instances, from 500 to 25 000 plates. This agreement, and also the agreement observed between the experimental results and the predictions of numerical solutions at moderate and high loading factors[40,41], confirm the validity of our numerical algorithm, and especially the soundness of the choice of the space and time integration increments for the proper simulation of the column efficiency (see above). The progressive change in band profile when the column efficiency (*i.e.*, the mass transfer coefficient) decreases is in excellent agreement also with the prediction of the kinetic model[12]. The band width, the thickness of the shock layer[22] and the band retention time increase while the band height decreases with decreasing column efficiency. The semi-equilibrium models cannot predict the changes in the band profile which take place when the mass transfer coefficient decreases further and the column efficiency becomes much lower than 500 theoretical plates. This problem is discussed elsewhere[1].

Figs. 17 and 18 compare the profiles derived from the Haarhoff–Van der Linde equation and from the numerical solution, with either a parabolic or a Langmuir

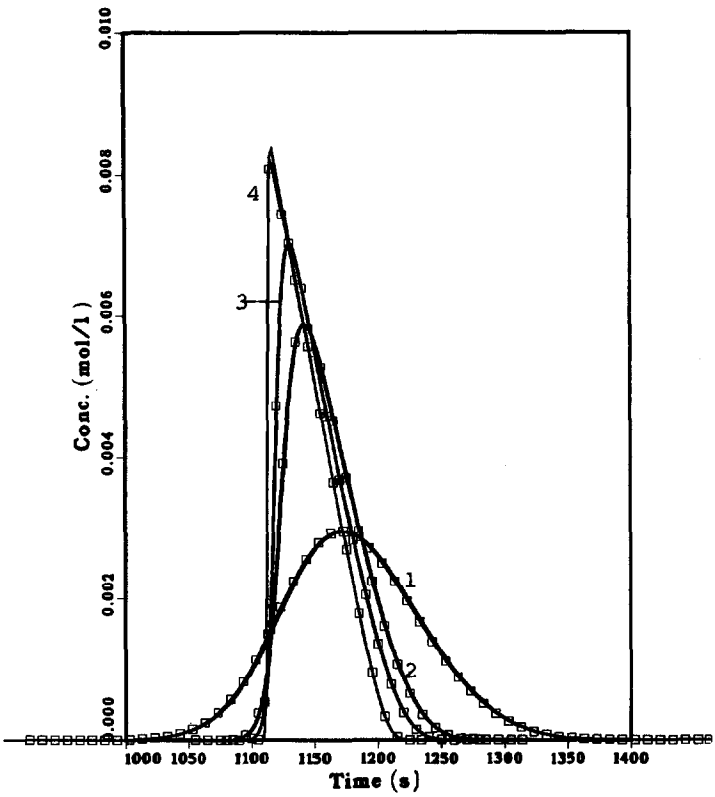

Fig. 16. Comparison between the band profiles predicted by the Haarhoff–Van der Linde equation and calculated by the numerical solution of the semi-ideal model. Parabolic isotherms, as for Fig. 1. Conditions as in Fig. 1, except loading factor, 0.2%, and variable column efficiency: (1) 500; (2) 2500; (3) 5000; (4) 25 000 plates. The Haarhoff–Van der Linde profiles are identified by squares.

isotherm, at loading factors of 1% (Fig. 17) and 5% (Fig. 18), for a 2500-plate column. In Fig. 18, the band profile derived from the Houghton equation is also shown. It is remarkable that at these high values of the loading factor the Haarhoff–Van der Linde profile is still in close agreement with the numerical solution calculated with a parabolic isotherm. This assumption, however, is unacceptable. Paradoxically, the Houghton equation, which is much less correct from a pure mathematical point of view, is in closer agreement with the correct profiles predicted by the numerical solution, in the case of a Langmuir isotherm, because of the nature of the systematic error which was introduced during its derivation (see above). Fig. 18 explains the observation reported by Wade and Carr[52] that better fits of experimental band profiles are obtained when using the Houghton equation than with the Haarhoff–Van der Linde equation, although the former is less correct, as it does not even conserve mass.

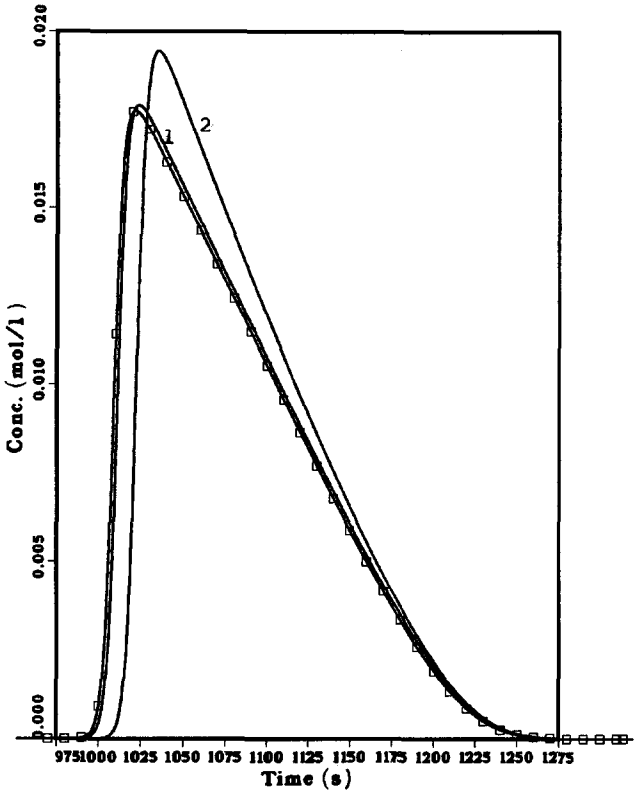

Fig. 17. Comparison between the band profiles predicted by the Haarhoff–Van der Linde equation and calculated by the numerical solution of the semi-ideal model. Influence of the isotherm. Conditions as in Figs. 7 and 8. Column efficiency, 2500 plates; loading factor, 1%. (1) Profile calculated with the numerical solution using a parabolic isotherm; (2) profile calculated by the numerical solution using a Langmuir isotherm. The Haarhoff–Van der Linde profile is identified by squares.

Comparison between the analytical solution of the ideal model and the numerical solutions of the semi-ideal model

We now compare the profile given by the analytical solution of the ideal model and the profile calculated using the numerical solution of the semi-ideal model (eqn. 12) for the same isotherm. This will permit a discussion of the validity of the ideal model and of the kinetic correction which has been described above.

Fig. 19 shows a comparison between the two profiles for a Langmuir isotherm, with loading factors between 0.5 and 20%. The reduced sample size, m (eqn. 34), varies from 7 to 280. The agreement between the two solutions corresponding to the same loading factor improves with increasing loading factor. The ideal model becomes a good approximation of the actual profile when m exceeds 35, as explained above.

Fig. 20 compares the profiles calculated by using the numerical solution of the semi-ideal model and the analytical solution of the ideal model, for different column efficiencies and loading factors, corresponding to a common value of $m = 35$. The agreement between each pair of profiles improves with increasing column efficiency,

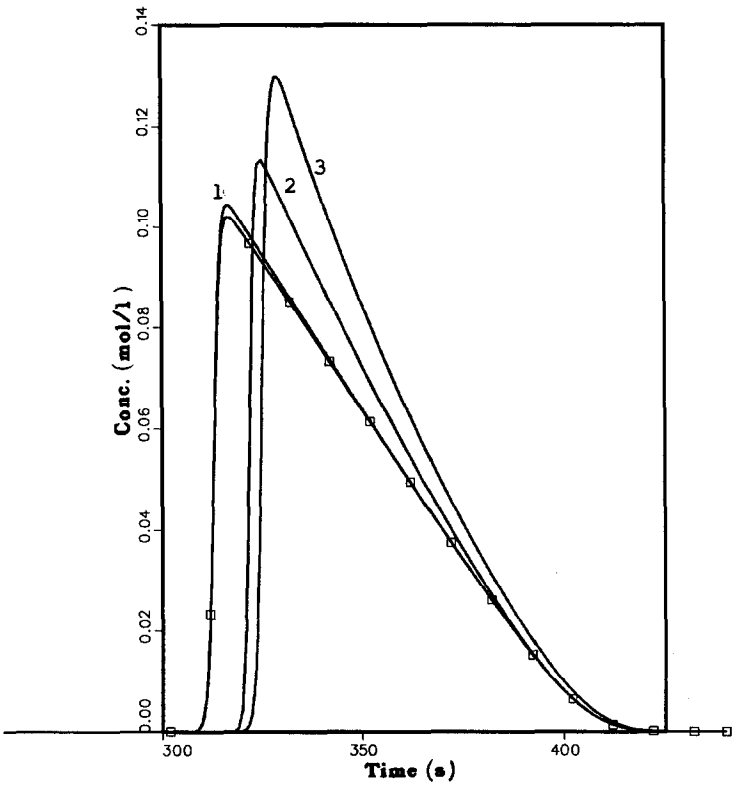

Fig. 18. Comparison between the band profiles predicted by the Haarhoff–Van der Linde and the Houghton equations and calculated by the numerical solution of the semi-ideal model. Influence of the isotherm. Conditions as in Figs. 7 and 8. Column efficiency, 2500 plates; loading factor, 5%. (1) Profile calculated with the numerical solution using a parabolic isotherm; (2) profile derived from the Houghton equation; (3) profile calculated by the numerical solution using a Langmuir isotherm. The Haarhoff–Van der Linde profile is identified by squares.

i.e., with decreasing loading factor at constant m. A similar result has been shown in Fig. 4, when comparing the Haarhoff–Van der Linde profile and the solution of the ideal model for a parabolic isotherm. It is much more apparent in the present case, however. Even at large values of the loading factor (*e.g.*, 10%), there is still a marked difference between the solutions of the ideal and semiideal model when the column efficiency is poor.

SOLUTIONS OF THE EQUILIBRIUM MODELS FOR A TWO-COMPONENT MIXTURE

The main purpose of chromatography is to separate and purify substances, not to elute single-component bands. The solution of the single-compound band profile is useful because it is the simplest non-linear chromatographic problem, so, if we cannot solve it, we cannot possibly discuss properly a multi-component problem. Further, the solution of the single-compound problem tells us how high concentration bands

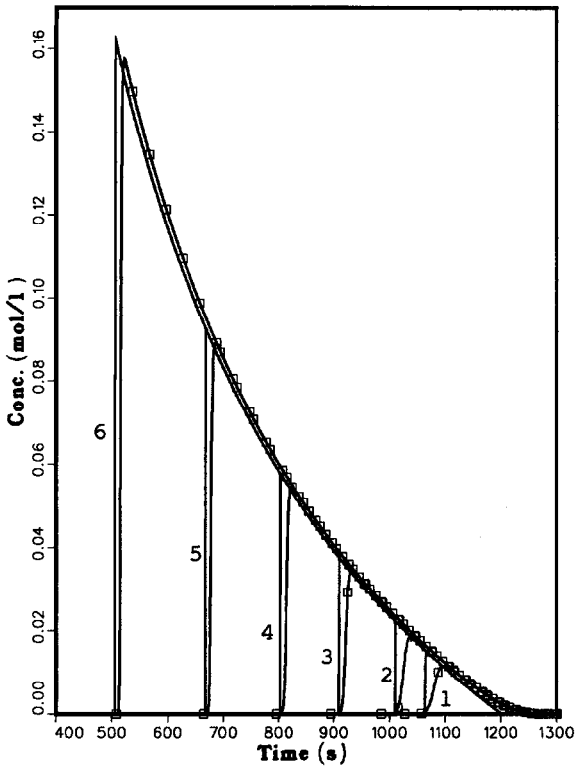

Fig. 19. Comparison between the band profiles predicted by the analytical solution of the ideal model and the numerical solution of the semi-ideal model. Influence of the loading factor at constant plate number. Conditions as in Fig. 1, except corresponding Langmuir isotherm. Column efficiency, 2000 theoretical plates. Loading factors (L_t) and reduced sample size (m): (1) 0.5%, 7; (2) 1%, 14; (3) 2.5%, 35; (4) 5%, 70; (5) 10%, 140; (6) 20%, 280.

migrate in chromatographic columns and how their profiles are affected by the non-linear behavior of the equilibrium isotherm. This solution emphasizes the main problems we are faced with when attempting to deal with the second simplest problem of non-linear chromatography, the two-component problem. There is one complicating factor, however, and it is of major importance: under non-linear conditions, the amount of one component in the stationary phase at equilibrium with a multicomponent solution is a function of the concentrations of *all* the components. The solution of the two-component problem therefore requires the consideration of binary or competitive isotherms.

Semi-ideal model

It is simple and straightforward to extend to the two-component problem the formulation of the single-compound problem and to show that, provided the mass transfer kinetics are fast enough and the column efficiency exceeds a few hundred plates, the elution band profiles of each component will be solutions of the following system of partial differential equations:

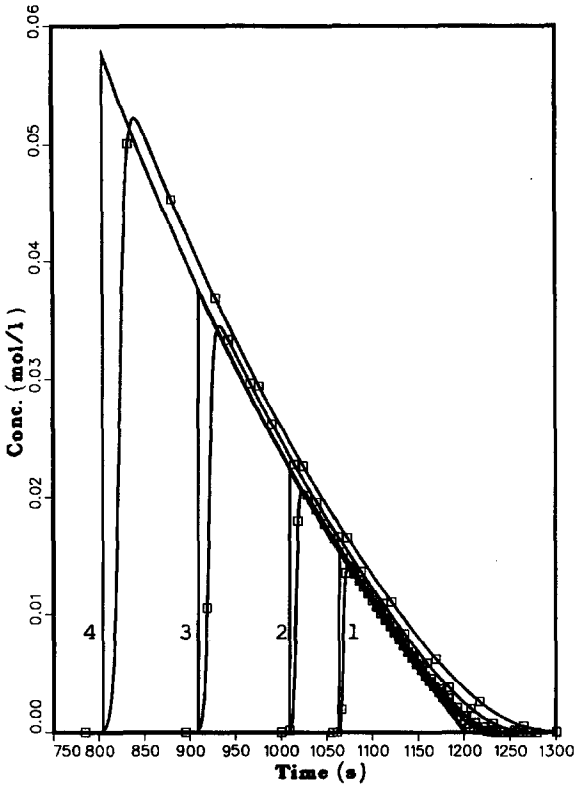

Fig. 20. Comparison between the band profiles predicted by the analytical solution of the ideal model and the numerical solution of the semi-ideal model. Influence of plate number at constant reduced sample size (m = 35). Conditions as in Fig. 1, except corresponding Langmuir isotherm. Column efficiencies and loading factors: (1) N = 10 000, L_f = 0.5%; (2) N = 5000, L_f = 1%; (3) N = 2000, L_f = 2.5%; (4) N = 1000, L_f = 5%.

$$\frac{\partial C_1}{\partial t} + F\frac{\partial q_1}{\partial t} + u\frac{\partial C_1}{\partial x} = D_a\frac{\partial^2 C_1}{\partial z^2} \tag{47}$$

and

$$\frac{\partial C_2}{\partial t} + F\frac{\partial q_2}{\partial t} + u\frac{\partial C_2}{\partial x} = D_a\frac{\partial^2 C_2}{\partial z^2} \tag{48}$$

In these equations, q_1 and q_2 are given by

$$q_i = f_i(C_1, C_2) \qquad i = 1,2 \tag{49}$$

Because of the competition between the two components of the mixture for interaction with the stationary phase, the two-component problem is much more complex than the

single-compound problem. The mass balance equations of the two components, 1 and 2, are coupled by the binary isotherm equations.

Thus, neither the analytical solutions of the semi-equilibrium models (the Houghton[36] and Haarhoff–Van der Linde[20] equations) nor those of the kinetic models (Thomas[6], Goldstein[7] and Wade *et al.*[8] models) can be extended to the solution of the two-component problem. The mathematical difficulties to be faced in order to solve the system of eqns. 47–49 are too formidable to be tackled with second-degree partial differential equations. The system of equations corresponding to the ideal model (*i.e.*, an infinite column efficiency, and $D_a = 0$ in eqns. 47 and 48), which is much simpler, can be solved, however (see next section). Under conditions when the ideal model does not give satisfactory results (values of m too small), a numerical solution can be obtained by extending the approach described above to the system of eqns. 47–49.

Analytical solution of the ideal model

The solution of the ideal model for two components has been discussed by Offord and Weiss[53] and by Glueckauf[26]. Both obtained very important, but incomplete results. Helfferich and Klein[54] developed a theory of multi-component ideal chromatography based on the use of the concept of coherence and of the h-transform. They obtained results which are in agreement with those of the shock theory[28]. Most of their work dealt with the application of this method to the investigation of displacement and frontal analysis. They published distance–time diagrams which describe the migration process, the dilution and the progressive separation of a pulse of a binary mixture, with competitive Langmuir isotherms.

Recently, we published an analytical solution of the two-component elution problem, in the case of binary Langmuir equilibrium isotherms, based on the use of the characteristic theory and the shock theory[33]. We have also been able to derive the same equations from the previous results obtained by Helfferich and Klein, using the h-transform method[34]. Both results are based on the use of the Langmuir competitive isotherm equation:

$$q_i = \frac{a_i C_i}{1 + b_1 C_1 + b_2 C_2} \tag{50}$$

It has not been possible yet to extend this approach to other isotherm equations, however, as was done in the case of the single compound problem[32]. We have also extended to the case of the two-component problem the use of the numerical algorithm derived for the solution of the semi-ideal[55] and the kinetic[13] models of chromatography.

In the case of a single solute, with a convex upward isotherm, a concentration discontinuity or shock is formed when a rectangular sample pulse enters the column[22]. The continuous, simple wave solution accounts for the rear of the profile. The band top belongs to both solutions, the shock and the simple wave[31]. It turns out that its velocity as a point on the simple wave solution is higher than the shock velocity. Hence, the shock is eroded and decreases. With a two-component sample, the situation is more complex. The less strongly adsorbed component moves ahead of the more strongly

adsorbed component. Two shocks appear, one at the front of the first component band and the second at the front of a mixed band. Two simple wave solutions take place, one for the pure second component and one for the mixed band. The development of the chromatogram and the progressive separation between the two bands can be understood by using the shock theory and the simple wave theory, which describe their behavior and their interference[33].

A characteristic feature of the solution of the ideal model is the concentration plateau on the rear of the second component profile. This plateau had already been predicted by Glueckauf[26]. It results from the fact that, in the ideal model, a velocity can be associated with each concentration. This velocity is a function of the concentration[22,28] and, with convex upward isotherms, increases with increasing concentration. As can be expected, the theory predicts that the velocity associated with a concentration of the second component in the presence of the first component decreases with decreasing concentration of this first component, when the isotherm is a competitive Langmuir isotherm. However, theory predicts that the velocity associated with the concentration of the second component tends towards a limit when the concentration of the first component tends towards zero at the end of the mixed band. This limit velocity is higher than the velocity associated with the same concentration of the pure second component. As a result, the second component leaks out of the intermediate, mixed band at a constant concentration, hence a concentration plateau arises. The length and the concentration of this plateau depend on the feed composition; the former increases and the latter decreases with decreasing proportion of the second component in the feed.

The chromatogram includes three zones. The third zone contains the pure second component. The rear part of its profile is the same as if the second component were alone. It ends at $t^0_{R,2} + t_p$, and begins at the concentration plateau. In the second zone the two components coexist. The first zone contains the first component, confined between the two shocks.

The analytical solution of the ideal model is relatively simple, but it appears complex because it is made of seven different points, four arcs, two concentration discontinuities and one concentration plateau (see Fig. 21). The coordinates of the seven feature points and the equations of the four arcs are given in Tables I–III, together with the definitions of the intermediate parameters used in these equations. The order of presentation of the solution emphasizes the fact that the chromatogram is anchored at its end ($t = t^0_{R,2} + t_p$) and that the solution is progressively derived by going backwards, from the end of the chromatogram towards the front.

Finally, we emphasize here that, if the two bands are separated when they leave the column, the profile of the second one is given by the same equation which gives the profile of a pure compound, but that *the same is not true for the first component*. The first component band conserves forever the memory of its interaction with the second component.

Comparison between the analytical solution of the ideal model and the numerical solution of the semi-ideal model

Fig. 22 shows a comparison between the band profiles calculated for the two components of a binary mixture using the numerical solution and the profiles given by the equations in Tables II and III (ideal model). The coefficients of the competitive

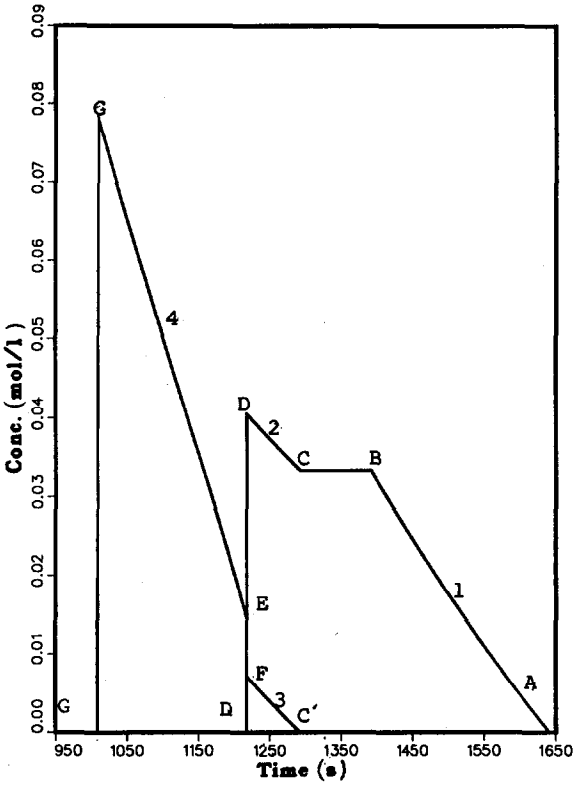

Fig. 21. Analytical solution of the ideal model for two components with competitive Langmuir isotherms. Relative composition of the mixture, 1:1. The coordinates of the points A–G and the equations of curves 1–4 are given in Table I.

Langmuir isotherms are given in the figure caption. The relative retention of the two components under linear conditions would be 1.20. The relative composition of the feed is 4:1. The column efficiency and sample size are such that the reduced sample size, m, is 120 for the first component and 30 for the second. The agreement between the two profiles is generally good, although some of the important features of the ideal model are smoothed out or totally eroded in the semi-ideal model numerical solution. For example, the second shock has totally disappeared from the rear of the first component profile, and the shock layer on the front of the second component is very thick and is also shorter than predicted. Nevertheless the broadening of the second band takes place much as predicted by the ideal model, and the result, the tag-along effect, would have been unpredictable from the mere consideration of the theory of the single compound profile. Fig. 23 compares the band profiles predicted by the ideal model under the same experimental conditions as for Fig. 22, with the numerical solution obtained under conditions where m is 24 for the first component and 6 for the second. The second component band is now nearly Gaussian and the first component band is markedly broadened and smoothed. The ideal model, which predicted correctly the

TABLE I

DEFINITIONS

Langmuir equilibrium isotherms:

$$q_i = a_i C_i/(1 + b_1 C_1 + b_2 C_2)$$

where q_i and C_i are the concentrations of component i at equilibrium in the stationary and the mobile phases, respectively

Relative retention:

$$\alpha = a_2/a_1$$

Constant γ:

$$\gamma = \frac{\alpha b_1 r_1 + b_2}{b_1 r_1 + b_2}$$

Roots of the Clairaut differential equation:

They are the roots, $r_1 > r_2$, of the following equation:

$$\alpha b_1 C_2^0 r^2 - (\alpha - 1 + \alpha b_1 C_1^0 - b_2 C_2^0) r - b_2 C_1^0 = 0$$

Loading factors:

$$L_f' = \left(1 + \frac{b_1 r_1}{b_2}\right) L_{f,2}$$

$$L_{f,2} = \frac{b_2 C_2^0 t_p}{t_{R,2}^0 - t_0} = \frac{b_2 n_2}{F_v(t_{R,2}^0 - t_0)} = \frac{b_2 n_2}{\varepsilon S L k'_{0,2}}$$

profiles at high values of the reduced sample size, m, gives a poor approximation at low values of m.

Similarly, Fig. 24 compares the band profiles obtained with the two procedures discussed, for a mixture of the same two components as for Fig. 22, but with a relative concentration of 1:4. The value of m corresponding to the sample size and the column efficiency is 30 for the first component and 120 for the second. There is excellent agreement with the profiles predicted by the two methods. The shock layers on the front of the two component profiles predicted by the numerical method are very thin, thinner than the shock layer at the rear of the first component. The plateau on the rear of the second component profile has been smoothed out by diffusion, and an inflection at the corresponding concentration is the only trace left. In Fig. 25, the corresponding values of m are only 6 and 24 for the first and second components, respectively, and as in Fig. 23 the agreement between the two profiles is poor. The interaction between the two bands is still obvious by the tail of the first component band.

Correction for the finite column efficiency

Using the analytical solution of the ideal model for two components[33], equations have been derived for the purity, the production rate and the recovery yields of these two components, as a function of the experimental parameters[56]. They permit the determination of the feed injection size and the cutting times for the maximum production rate of these compounds at any degree of stated purity.

A correction based on the same principle as that used for the single-compound profile has been derived recently[57]. This correction permits the investigation of the influence on the production rate of the column efficiency and of the dependence of this

TABLE II

COORDINATES OF THE CHARACTERISTIC POINTS OF THE CHROMATOGRAM IN FIG. 21

Point	*Coordinates*
A	$t_A = t_p + t^0_{R,2}$ $C_A = 0$
B	$t_B = t_0 + t_p + \frac{\gamma^2}{\alpha^2}(t^0_{R,2} - t_0)$ $C_B = \frac{\alpha - 1}{b_2 + \alpha b_1 r_1}$
C	$t_C = t_p + t_0 + \frac{\gamma}{\alpha}(t^0_{R,1} - t_0)$ $C_C = \frac{\alpha - 1}{b_2 + \alpha b_1 r_1}$
D	$t_D = t_p + t_0 + \gamma(t^0_{R,2} - t_0)(1 - \sqrt{L'_f})^2$ $C_D = \frac{1}{b_2 + \alpha b_1 r_1} \cdot \frac{\sqrt{L'_f}}{1 - \sqrt{L'_f}}$
E	$t_E = t_D$ $C_E = \frac{[(1 - \alpha)/\alpha] + \sqrt{L'_f}}{1 - \sqrt{L'_f}}$
F	$t_F = t_D$ $C_F = \frac{r_1}{b_2 + \alpha b_1 r_1} \cdot \frac{1 - \alpha + \alpha\sqrt{L'_f}}{1 - \sqrt{L'_f}}$
G	The retention time and the concentration of point G cannot be obtained in closed forms. The retention time is derived by calculating the lower boundary of the finite integral of the profiles of the first component (equations of lines 3 and 4, Table III and Fig. 21). This integral is equal to the mass injected of the first component. The concentration is then obtained by placing the retention time of the front shock in the equation of line 4. L'_f is defined in Table I.

efficiency on the flow velocity. The selection of the experimental conditions permitting the maximum production rate under a certain set of constraints (purity of the products or recovery yield) becomes possible. These results are in excellent agreement with those obtained from numerical solutions of the semi-ideal model. This confirms the validity of our approach[57].

TABLE III

EQUATIONS FOR THE CONTINUOUS PROFILES ON THE CHROMATOGRAM SHOW IN FIG. 21

Line	*Equation*
Line 1, AB	$C_{AB} = \frac{1}{b_2}\left[\sqrt{\left(\frac{t^0_{R,2} - t_0}{t - t_p - t_0}\right)} - 1\right]$
Line 2, CD	$C_2 = \frac{1}{b_2 + \alpha b_1 r_1}\left[\sqrt{\gamma \cdot \frac{t^0_{R,2} - t_0}{t - t_p - t_0}} - 1\right]$
Line 3, C'F	$C_1 = \frac{1}{b_1 + b_2/\alpha r_1}\left[\sqrt{\frac{\gamma}{\alpha} \cdot \frac{t^0_{R,1} - t_0}{t - t_p - t_0}} - 1\right]$
Line 4, EG	$t = t_p + t_0 + (t^0_{R,1} - t_0)\left\{\frac{1}{(1 + b_1 C_1)^2} - L_{f,2} \cdot \frac{\alpha - 1}{\alpha} \cdot \frac{1}{[(\alpha - 1)/\alpha + b_1 C_1]^2}\right\}$

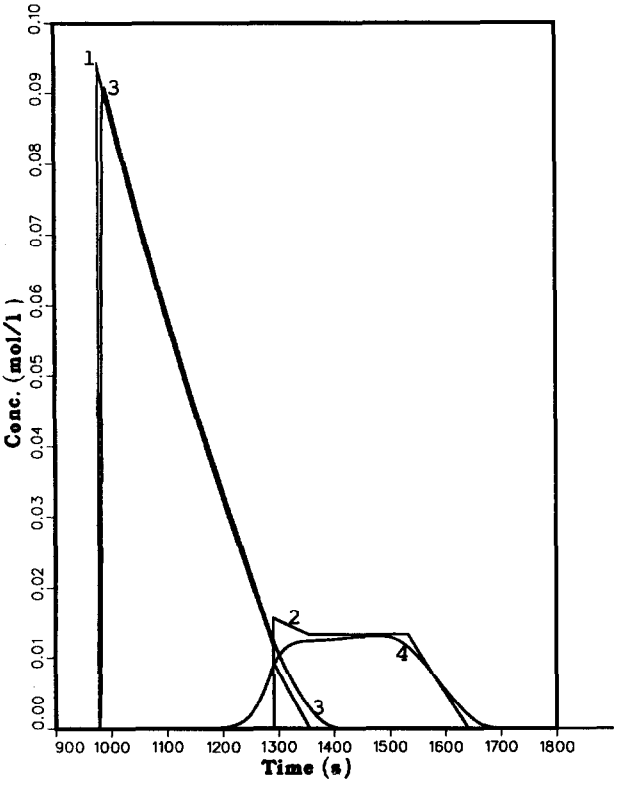

Fig. 22. Comparison between the elution band profiles of a two-component mixture calculated with the ideal model and with the numerical solution of the semi-ideal model. Langmuir competitive isotherm (eqn. 53), with $a_1 = 6$, $a_2 = 7.2$, $b_1 = 2.5$, $b_2 = 3.0$. Column length, 25 cm; dead time, $t_0 = 200$ s; column efficiency, 5000 theoretical plates; relative composition of the feed, 4:1; sample size, $L_{f,1} = 3.3\%$, $L_{f,2} = 0.83\%$. Profiles: (1) first component, ideal model; (2) second component; ideal model; (3) first component, numerical solution; (4) second component, numerical solution.

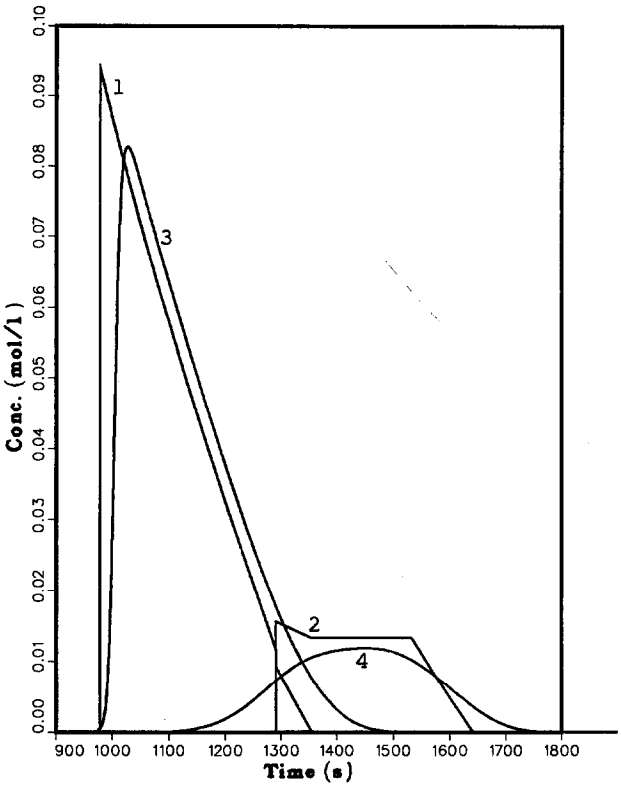

Fig. 23. Comparison between the elution band profiles of a two-component mixture calculated with the ideal model and with the numerical solution of the semi-ideal model. Conditions as in Fig. 22, except column efficiency, 1000 theoretical plates. Profiles: (1) first component, ideal model; (2) second component, ideal model; (3) first component, numerical solution; (4) second component, numerical solution.

CONCLUSION

Considerable progress have been made in the investigation of the fundamental problems of chromatography through the use of the equilibrium and semi-equilibrium models. There remain a few unsolved problems which deserve attention.

First, we still need a solution giving in closed form the equation of the elution profile of a single compound at large values of the loading factor. What we are really missing at present is an equation which would be, at high loading factors, the equivalent of the Haarhoff–Van der Linde equation at low sample sizes, an equation which would account fully for the thermodynamic effects and correct to the first order for the kinetic effects. Barring that, a practical and accurate correction of the solution of the ideal model, taking into account the smoothing effect of a finite column efficiency, would be highly valuable.

The two-component problem is much more difficult and less well understood than the single-compound problem. An extension to the case of other isotherms of the solution of the ideal model for two components which we have derived recently in the

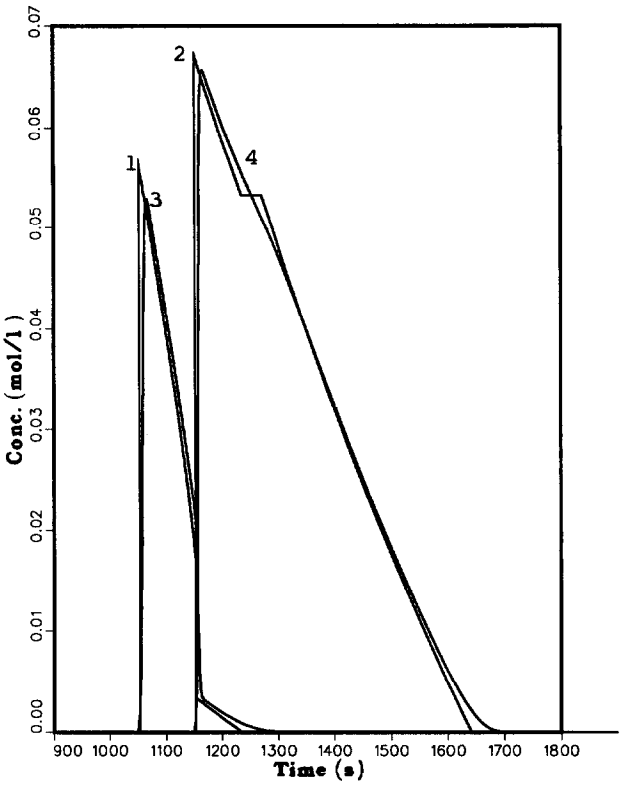

Fig. 24. Comparison between the elution band profiles of a two-component mixture calculated with the ideal model and with the numerical solution of the semi-ideal model. Conditions as in Fig. 23, except relative composition of the feed, 1:4. Profiles: (1) first component, ideal model; (2) second component, ideal model; (3) first component, numerical solution; (4) second component, numerical solution.

case of competitive Langmuir isotherms would be a further great progress. Admittedly, any progress in the understanding of the competitive behavior of the components of a mixture for adsorption (or, more generally, for interaction with the stationary phase) would be very valuable at this stage of development of non-linear chromatography. It may be that the lack of understanding of competitive isotherms is the most critical hindrance. An analytical solution of the semi-ideal model, valid at high concentrations, is needed in order to investigate in depth the various problems currently arising in connection with the optimization of the experimental conditions of preparative chromatography. At the very least, we need also a practical and accurate correction of the solution of the ideal model taking into account the effects of the finite column efficiency.

Finally, we have discussed so far only one part of the problem. The mass belance equations, the equations of the semi-ideal model, are non-linear, hyperbolic partial differential equations. They are non-linear because the coefficient of one of the partial differentials depends on the function [*i.e.*, the equilibrium isotherm, $f(C)$]. We have searched for solutions of these equations, knowing the function $f(C)$, and as we have

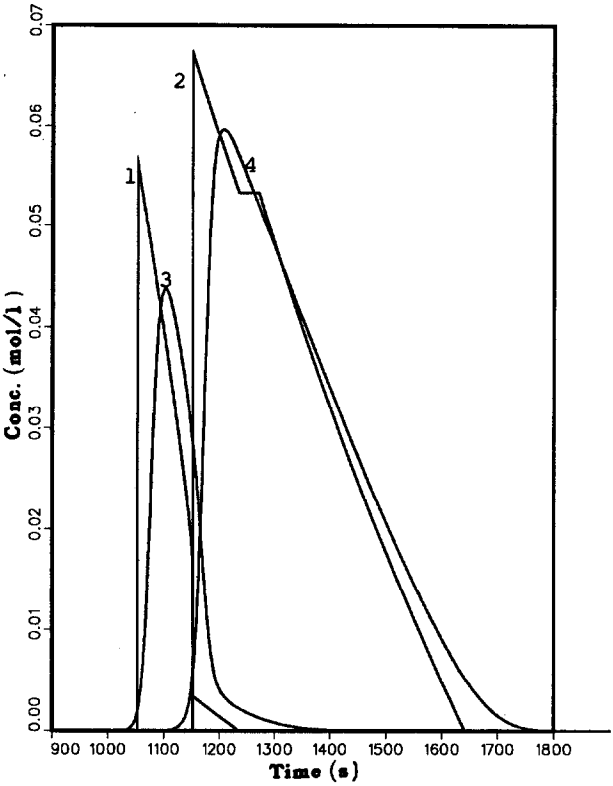

Fig. 25. Comparison between the elution band profiles of a two-component mixture calculated with the ideal model and with the numerical solution of the semi-ideal model. Conditions as in Fig. 24, except relative composition of the feed, 1:4. Sample size, $L_{f,1} = 0.83\%$, $L_{f,2} = 3.3\%$. Profiles: (1) first component, ideal model; (2) second component, ideal model; (3) first component, numerical solution; (4) second component, numerical solution.

seen it is a difficult task. Far more difficult, both from a theoretical viewpoint and in practice, is the converse problem of knowing solutions of the partial differential equation, finding access to the function in order to obtain an accurate estimate. This problem is at the forefront of mathematical research[58]. In many simpler problems, direct empirical procedures have been used with some success. The principle consists in starting from a crude multi-parameter estimate of the function, calculating the corresponding solution and using various computational techniques to minimize some measure of the distance between the band profile recorded experimentally and those calculated, in order to optimize the values of the parameter. Most probably, this approach cannot be entirely satisfactory. Methods having a more sound theoretical background are needed.

SYMBOLS

A Peak area (eqn. 30a)
a First coefficient of the Langmuir isotherm (eqn. 19)

b second coefficient of the Langmuir isotherm (eqn. 19)
C Concentration of the studied compound in the mobile phase (eqn. 1)
$C(z,t)$ Concentration of the studied compound in the mobile phase, at time t and position z (eqn. 5)
C_{Max} Maximum concentration in a chromatographic band (eqn. 18)
C_s Concentration of the studied compound in the stationary phase (eqn. 1)
C_0 Concentration of the compound in the feed (injected sample) (eqn. 5)
C_1,C_2 Concentrations of the two components of a binary mixture in the mobile phase (eqn. 47)
$\bar{C}$ Total concentration of the studied compound, referred to the total column volume (eqn. 11)
$\bar{C}_m$ Concentration of the studied compound in the mobile phase, referred to the total column volume (eqn. 8)
$\bar{C}_s$ Concentration of the studied compound in the stationary phase, referred to the total column volume (eqn. 8)
$\bar{C}_m^*$ Equilibrium concentration in the mobile phase, referred to the total column volume (eqn. 8)
$\bar{C}_s^*$ Equilibrium concentration in the stationary phase, referred to the total column volume (eqn. 8)
D Coefficient of axial dispersion (eqn. 1)
D_p Intraparticle diffusion coefficient (eqn. 7)
D' Pseudo-diffusion coefficient (eqn. 11)
D_a Apparent diffusion coefficient (eqn. 12)
d_p Average particle diameter of the packing (eqn. 7)
F Phase ratio (eqn. 1)
F_v Volume flow-rate of mobile phase (eqn. 17)
H Column HETP (eqn. 6)
H_{app} Observed column HETP (eqn. 44)
H_{th} Thermodynamic contribution to the column HETP (eqn. 44)
h Space integration increment in the numerical calculations of elution profiles (eqn. 46)
J Longitudinal flux of compound per unit cross-sectional area (eqn. 10)
k_a Adsorption rate constant (eqn. 2)
k_d Desorption rate constant (eqn. 2)
k_f Lumped mass transfer coefficient (eqn. 4)
k_1,k_2 Rate constants (eqn. 3)
k'_0 Column capacity factor at infinite dilution (eqn. 6)
k_e External film mass transfer coefficient (eqn. 7)
L Column length (eqn. 26)
L_f Loading factor for a compound (eqn. 11)
L'_f Auxiliary loading factor (Table I)
m Reduced sample size (eqn. 29)
N Limit efficiency for an infinitely small sample size (eqn. 34)
N_{app} Observed plate number of the column (eqn. 41)
N_{th} Plate number observed in non-linear chromatography with an ideal column (eqn. 38a)
n Sample size (eqn. 17)

q Concentration of a compound in the stationary phase in equilibrium with the concentration C_m in the mobile phase (eqn. 4); also isotherm equation (eqn. 13)
q_s Column saturation capacity (eqn. 2)
R Fraction of a solute in the mobile phase (eqn. 11)
S Column cross-sectional area (eqn. 26)
t time (eqn. 1)
t_0 Column dead time (eqn. 15)
t_p Duration of the injection of the sample (eqn. 5)
t_R Retention time (eqn. 17)
$t_{R,0}$ Retention time at infinite dilution (eqn. 16)
u Mobile phase velocity (eqn. 1)
W_{th} Baseline band width of the band profile predicted by the ideal model (eqn. 38)
X Reduced concentration in the solution of the Houghton equation (eqn. 29)
z length (abscissa) along the column (eqn. 1)
β Inner porosity of the packing particles (eqn. 7)
ΔJ Contribution to the longitudinal flux of a compound due to non-equilibrium (eqn. 11)
ε Packing porosity (eqn. 1)
$\varepsilon_m, \varepsilon_s$ Relative deviation from equilibrium (eqn. 8)
Λ Reduced variable in the Houghton equation (eqn. 28)
ξ Reduced variable in the Houghton equation (eqn. 28)
τ Reduced time in the Houghton equation (eqn. 29); also time integration increment in the calculation of elution profiles (eqn. 46)

ACKNOWLEDGEMENTS

This work was supported in part by Grant CHE-8901382 of the National Science Foundation and by the cooperative agreement between the University of Tennessee and the Oak Ridge National Laboratory.

REFERENCES

1 S. Golshan-Shirazi and G. Guiochon, in preparation.
2 J. N. Wilson, *J. Am. Chem. Soc.*, 62 (1940) 1583.
3 G. Guiochon, S. Golshan-Shirazi and A. Jaulmes, *Anal. Chem.*, 60 (1988) 1856.
4 S. Golshan-Shirazi and G. Guiochon, *J. Chromatogr.*, 461 (1989) 1.
5 E. sz. Kováts, in F. Bruner (Editor), *The Science of Chromatography*, Elsevier, Amsterdam, 1985, p. 205.
6 H. C. Thomas, *J. Am. Chem. Soc.*, 66 (1944) 1664.
7 S. Goldstein, *Proc. R. Soc. London, Ser. A*, 219 (1953) 151.
8 J. L. Wade, A. F. Bergold and P. W. Carr, *Anal. Chem.*, 59 (1987) 1286.
9 L. Lapidus and N. R. Amundson, *J. Phys. Chem.*, 56 (1952) 984.
10 E. Glueckauf and J. I. Coates, *J. Chem. Soc.*, (1947) 1315.
11 N. K. Hiester and T. Vermeulen, *Chem. Eng. Prog.*, 48 (1952) 505.
12 B. Lin, S. Golshan-Shirazi and G. Guiochon, *J. Phys. Chem.*, 93 (1989) 3363.
13 S. Golshan-Shirazi, B. Lin and G. Guiochon, *J. Phys. Chem.*, 93 (1989) 6871.
14 J. J. Van Deemter, F. J. Zuiderweg and A. Klinkenberg, *Chem. Eng. Sci.*, 5 (1956) 271.
15 A. J. P. Martin and R. L. M. Synge, *Biochem. J.*, 35 (1941) 1359.
16 E. Kucera, *J. Chromatogr.*, 19 (1965) 237.
17 C. Horvath and H. J. Lin, *J. Chromatogr.*, 149 (1978) 43.
18 J. F. K. Huber, *Ber. Bunsenges. Phys. Chem.*, 77 (1973) 179.
19 J. C. Giddings, in *Dynamics of Chromatography*, Marcel Dekker, New York, 1965.

20 P. C. Haarhoff and H. J. Van der Linde, *Anal. Chem.*, 38 (1966) 573.
21 D. DeVault, *J. Am. Chem. Soc.*, 65 (1943) 532.
22 B. Lin, S. Golshan-Shirazi, Z. Ma and G. Guiochon, *Anal. Chem.*, 60 (1988) 2647.
23 J. Weiss, *J. Chem. Soc.*, (1943) 297.
24 E. Glueckauf, *J. Chem. Soc.*, (1947) 1302.
25 E. Glueckauf, *Nature (London)*, 156 (1945) 205.
26 E. Glueckauf, *Proc. R. Soc., London, Ser. A*, 186 (1946) 35.
27 H. K. Rhee, R. Aris and N. R. Amundson, *Philos. Trans. R. Soc. London, Ser. A*, 267 (1970) 419.
28 R. Aris and N. R. Amundson, *Mathematical Methods in Chemical Engineering*, Prentice Hall, Englewood Cliffs, NJ, 1973.
29 G. Guiochon and L. Jacob, *Chromatogr. Rev.*, 14 (1971) 77.
30 P. Valentin and G. Guiochon, *Sep. Sci.*, 10 (1975) 245.
31 S. Golshan-Shirazi and G. Guiochon, *Anal. Chem.*, 60 (1988) 2364.
32 S. Golshan-Shirazi and G. Guiochon, *J. Phys. Chem.*, 94 (1990) 495.
33 S. Golshan-Shirazi and G. Guiochon, *J. Phys. Chem.*, 93 (1989) 4143.
34 S. Golshan-Shirazi and G. Guiochon, *J. Chromatogr.*, 484 (1989) 125.
35 B. Lin, Z. Ma and G. Guiochon, *Sep. Sci. Technol.*, 24 (1989) 809.
36 G. Houghton, *J. Phys. Chem.*, 67 (1963) 84.
37 A. Jaulmes, C. Vidal-Madjar, A. Ladurelli and G. Guiochon, *J. Phys. Chem.*, 88 (1984) 5379.
38 A. Jaulmes, C. Vidal-Madjar, H. Colin and G. Guiochon, *J. Phys. Chem.*, 90 (1986) 207.
39 A. Jaulmes, M. J. Gonzalez, C. Vidal-Madjar and G. Guiochon, *J. Chromatogr.*, 387 (1987) 41.
40 S. Golshan-Shirazi, S. Ghodbane and G. Guiochon, *Anal. Chem.*, 60 (1988) 2630.
41 S. Golshan-Shirazi and G. Guiochon, *Anal. Chem.*, 60 (1988) 2634.
42 J. H. Knox and H. M. Pyper, *J. Chromatogr.*, 363 (1986) 1.
43 S. Golshan-Shirazi and G. Guiochon, *Anal. Chem.*, 61 (1989) 462.
44 H. Poppe and J. C. Kraak, *J. Chromatogr.*, 255 (1983) 395.
45 J. E. Eble, R. L. Grob, P. E. Antle and L. R. Snyder, *J. Chromatogr.*, 384 (1987) 25.
46 J. E. Eble, R. L. Grob, P. E. Antle and L. R. Snyder, *J. Chromatogr.*, 384 (1987) 45.
47 J. C. Giddings, in E. Heftmann (Editor), *Chromatography*, Van Nostrand Rheinhold, New York, 3rd ed., 1975, p. 27.
48 A. M. Katti and G. Guiochon, *J. Chromatogr.*, 499 (1990) 21.
49 B. Lin and G. Guiochon, *Sep. Sci. Technol.*, 24 (1989) 31.
50 B. Lin, Z. Ma and G. Guiochon, *J. Chromatogr.*, 484 (1989) 83.
51 P. Rouchon, M. Schonauer, P. Valentin and G. Guiochon, *Sep. Sci.*, 22 (1987) 1793.
52 J. L. Wade and P. W. Carr, paper presented at PREP'89, VIth International Symposium on Preparative Chromatography, Washington, DC, May 9–11, 1989.
53 A. C. Offord and J. Weiss, *Nature (London)*, 155 (1945) 725.
54 F. Helfferich and G. Klein, *Multi-Component Chromatography. Theory of Interferences*, Marcel Dekker, New York, 1970.
55 G. Guiochon and S. Ghodbane, *J. Phys. Chem.*, 92 (1988) 3682.
56 S. Golshan-Shirazi and G. Guiochon, *Anal. Chem.*, 61 (1989) 1276.
57 S. Golshan-Shirazi and G. Guiochon, *Anal. Chem.*, 61 (1989) 1368.
58 V. G. Romanov, *Inverse Problems of Mathematical Physics*, VNU Science Press, Utrecht, 1987.